



3 1176 00072 0368

13 JAN 1948

UNCLASSIFIED

NACA RM No. A7130



H. L. Dryden 9-16-52

RESEARCH MEMORANDUM

for NACA Release form #783.
By HSR, 10-22-52

AN EXPERIMENTAL INVESTIGATION OF THE DESIGN VARIABLES
FOR NACA SUBMERGED DUCT ENTRANCES

By Emmet A. Mossman and Lauros M. Randall

Ames Aeronautical Laboratory
Moffett Field, Calif.

*MISSING
last
page
no longer
found in
ACR 5120*

CLASSIFICATION CANCELLED

Authority J. W. Cronley 1-13-54 #1
E.O. 10576

By [Signature] 1-14-54 See NACA
R 72156

This document contains classified information affecting the National Defense of the United States within the meaning of the Espionage Act, USC 1831 and 1832. Its transmission or the revelation of its contents in any manner to an unauthorized person is prohibited by law. Information so classified may be imparted only to persons in the military and naval services of the United States, appropriate civilian officers and employees of the Federal Government who have a legitimate interest therein, and to United States citizens of known loyalty and character who of necessity must be informed thereof.

NATIONAL ADVISORY COMMITTEE FOR AERONAUTICS

WASHINGTON

January 8, 1948

NACA LIBRARY

LANGLEY MEMORIAL AERONAUTICAL
LABORATORY
Langley Field, Va.

~~CONFIDENTIAL~~

~~RESTRICTED~~
~~CONFIDENTIAL~~
NATION

UNCLASSIFIED

NATIONAL ADVISORY COMMITTEE FOR AERONAUTICS

RESEARCH MEMORANDUMAN EXPERIMENTAL INVESTIGATION OF THE DESIGN VARIABLES
FOR NACA SUBMERGED DUCT ENTRANCES

By Emmet A. Mossman and Lauros M. Randall

SUMMARY

Information concerning the parameters and design variables affecting an NACA submerged duct design is presented. The principal variables investigated include entrance width-to-depth ratio, ramp-wall divergence, ramp angle, and deflector size. Tests were also made to show the effect of variation of boundary-layer thickness and ramp-floor contour.

Pressure recovery at the duct entrance and after slight diffusion, pressure distribution over the lip and ramp, and drag are given as functions of the inlet velocity ratio of the entrance. An evaluation of the NACA submerged entries indicates that satisfactory duct characteristics may be found for a range of the test variables. It appears that an optimum NACA submerged inlet design should employ curved diverging ramp walls, a 5° to 7° ramp angle, and a width-to-depth ratio of from 3 to 5. The boundary-layer thickness of the surface into which the inlet is placed was found to have a large effect on the pressure recovery.

Possible applications of this type of inlet and their particular advantages are discussed.

INTRODUCTION

For the development of a satisfactory air-induction system of an aircraft, several aerodynamic criteria must be evaluated in conjunction with those involving structural design and installation. Aerodynamically, the system should not reduce the available energy of the entering air, the drag of the body into which it is placed should not be increased, and the high-speed characteristics of the body or aircraft should not deteriorate. Although, in practice, an air-induction system possibly does not meet all these requirements, the merits of a system can be determined by the degree to which its characteristics approach the optimum.

~~RESTRICTED~~
~~CONFIDENTIAL~~
SECURITY INFORMATION

UNCLASSIFIED

A previous investigation of an air intake submerged below the body surface (reference 1) was exploratory in nature and was meant to indicate the trend for future research of this type inlet. This present report gives the results of more extensive investigations of NACA submerged duct entrances conducted at the Ames Aeronautical Laboratory. The work includes further development of certain configurations found to be desirable from preliminary tests and the investigation of other design parameters not previously considered.

SYMBOLS

A	duct-entrance area, square feet
B	distance ramp floor is submerged below reference contour at station where entrance area is measured
C_{DD}	duct drag coefficient $\left(\frac{D}{qA}\right)$
D	drag, pounds
d	duct depth
H	total pressure, pounds per square foot
ΔH	loss in total pressure, pounds per square foot
M	mach number
M_{CR}	critical Mach number
P	pressure coefficient $\left(\frac{p - p_0}{q_0}\right)$
p	static pressure, pounds per square foot
q	dynamic pressure $\left(\frac{1}{2}\rho V^2\right)$, pounds per square foot
U	velocity outside boundary layer, feet per second
u	local velocity in boundary layer, feet per second
V	velocity, feet per second
w	duct width
ρ	air density, slugs per cubic foot

η_D diffuser efficiency $\left(\frac{H_2 - P_1}{H_1 - P_1} \right) \times 100$, percent

$$(1 + \eta) \quad 1 + \frac{M^2}{4} + \frac{M^4}{40} + \frac{M^6}{1600} - \frac{M^8}{80,000} \dots$$

$H - p$ $q(1 + \eta)$, ram pressure, pounds per square foot

$\frac{H - P_0}{H_0 - P_0}$ ram recovery ratio

V_1/V_0 inlet-velocity ratio

Subscripts

- o free stream
- 1 duct-entrance station
- 2 station after diffusion

MODEL AND APPARATUS

Various models of submerged-duct entrances were tested in the Ames 8- by 36-inch wind tunnel of the 7- by 10-foot wind-tunnel section, which is shown schematically on figure 1. Each entrance to be investigated was placed in a removable portion of one of the 36-inch walls of the test section, this wall thus simulating the fuselage skin for a typical submerged-inlet application. Air was drawn through the inlet by a constant-speed centrifugal pump, the quantity flow being measured by a calibrated venturi and regulated by a motor-controlled plug-type valve located at the pump exit. The tests were made at tunnel speeds ranging from 180 to 260 feet per second.

All parts of the entrances for the greater portion of the investigation were flush with or below the surface of the tunnel wall. The area of the various entrances was held constant at 16 square inches and the width-to-depth ratio varied from 1 (4- by 4-inch) to 6 (9.81- by 1.64-inch). A separate model was required to test each of the six width-to-depth ratios. (See fig. 2.)

For each model four ramp plan forms were investigated (fig. 3). Ramp angle could be varied from 5° to 15° . Figure 4 shows the geometric change of the ramp with ramp angle for one entrance configuration. Provision was also made for testing a curved ramp floor shape, with the $w/d = 4$ entrance for ramp lengths which corresponded

to the 5°, 7°, 9°, and 11.5° straight ramp floors. This curved ramp floor, shown on figure 5, represented the upper-surface profile shape of the aft portion of a 65-series low-drag airfoil.

Deflectors, or small ridges along the top edge of the ramp wall with heights of 0.25, 0.50, 0.75, and 1.00 inch and lengths of 25, 50, 75, and 100 percent of the ramp length were tested (fig. 6).

The basic lip shape (fig. 7) was the same for all models, but the dimensions of the lip varied directly as the depth of the duct entrance. In every case the lip incidence could be varied through an angle range of $\pm 5^\circ$.

The models included a transition section which simulated an internal duct system with gradual diffusion. This section started 8 inches aft of the lip leading edge and for each model transformed from the rectangular cross section of the submerged duct inlet to a circular cross section 5.25 inches in diameter. The transition section was 36 inches long with a 1.35 expansion in area, constant for all models.

Rakes of pressure tubes for measuring ram recovery were located at two stations (fig. 2), one at the duct entrance and the other after diffusion in the 5.25-inch-diameter circular section. The rakes located at the entrance contained 64 evenly spaced total-pressure tubes and 4 static-pressure tubes. These rakes were mounted slightly behind the leading edge of the lip in each case at a station where the lip inner contour faired into a constant area section. The rake aft of the diffuser section had 33 total pressure tubes and 4 static-pressure tubes. The wind-tunnel air downstream of the inlet was surveyed by a series of individual rakes, located 8 inches aft of the lip station, which completely bracketed the wake caused by the entrance. Each of the individual rakes contained 15 tubes and were located at 8 spanwise stations.

Pressure distributions were obtained from small flush static-pressure orifices built into the submerged duct entrances along the center lines of the lip and ramp and also along a section of the lip 1 inch from the side wall of the entrance.

TESTS

To aid in the analysis of the data it was necessary to evaluate the existing testing conditions. The boundary layer of the test section tunnel wall, measured at the duct-entrance station, is given on figure 8. It should be noted that this boundary layer is considerably thicker than would be normally experienced if a submerged

entrance were located at or forward of the wing on a similarly scaled fuselage. Efforts to reduce this natural boundary-layer thickness did not prove successful, due mainly to the wind-tunnel geometry. The ratio of total boundary-layer thickness to duct depth ($w/d = 4$) is 0.80 for these tests as compared to 0.31 for a typical fighter installation (station 0, reference 2). From this it is evident that the pressure recoveries presented in this report must not be considered as the maximum values obtainable with NACA submerged duct entries. The lips of all models of the submerged entrance were located at the same position along the test section wall.

To determine the diffuser or internal duct efficiencies, bench tests of the six diffusers were made. A cone was attached to the entrance in place of the ramp and lip to assure satisfactory flow conditions. The pressure losses were measured aft of the diffusers in the circular portion of the diffuser at the same location and with the same rake that was used to determine the pressure recovery aft of the diffusers in the wind-tunnel tests. Results of these tests (fig. 9) show the efficiencies (η_D) of all six diffusers to be about 91 percent.

The principal parameters investigated in the wind tunnel were ramp plan form, width-to-depth ratio, ramp angle, and deflectors. A limited number of tests was made to show the effect of variation of ramp-floor contour and boundary-layer thickness at the location of the duct entrance. For evaluation of the relative merits of the various configurations measurements were taken to determine the pressure recovery aft of the diffuser section and at the entrance, pressure distribution on the lip and ramp, and drag of the configurations, through a range of inlet velocity ratios from 0 to 1.5.

Tables I and II are indices showing the range of modifications to the submerged duct entry.

RESULTS AND DISCUSSION

This investigation to obtain data for the development and application of NACA submerged-duct entries was concerned with the effect of various configuration changes upon the degree of fulfillment of the criteria set forth. The measurements necessary for evaluation, as mentioned previously, were pressure recovery after diffusion and at the entrance, pressure distribution, and drag. Under these categories the following parameters are discussed:

1. Ramp plan form

2. Width-to-depth ratio
3. Ramp angle
4. Ramp floor shape
5. Boundary-layer thickness

Because of the nature of the investigation, the results and discussion of deflectors are presented separately from the other divisions at the conclusion of this section.

A figure guide is given in table III. Only the more pertinent drag and pressure-distribution results are presented, the greater portion of the data being given in terms of pressure recovery.

Pressure Recovery

On this type inlet the velocity distribution is not uniform over the entrance area, and determining the entrance losses (Appendix A) becomes a difficult process. Consequently, a large portion of the data is evaluated from consideration of the pressure recovery after diffusion. Since the diffuser efficiencies from bench tests are equal, a comparison, for two inlet configurations, of the results after diffusion is a direct measure of their relative merits with respect to pressure recovery. This comparison, of course, includes the effect of the inlet on the diffuser efficiency. Entrance pressure recovery was obtained only for the most important values of the design parameters.

Pressure Recovery after Diffusion.-

Ramp plan form.- The results of previous investigations (references 1 and 2) showed that the ram pressure recovery of the submerged duct entrance could be appreciably increased by diverging the walls of the ramp. The effect of ramp plan form is shown in figure 10, which gives the pressure recovery measured after the diffuser section for two width-to-depth ratios. In all cases the curved diverging ramp which was previously developed (reference 1) gave the highest ram pressure recovery for the low inlet-velocity-ratio range ($V_1/V_0 \leq 0.6$). However, the effect of ramp plan form is also a function of width-to-depth ratio and ramp angle and will be discussed in later sections.

In the instances where the pressure recovery is increased by diverging the ramp plan form, the process is apparently one

of diverting the boundary layer outside the ramp around the entrance. Experimental data show this possibly to be due to two causes. The first is indicated from a comparison of the ramp pressure distribution with that on the surface in the immediate proximity of the entrance. These pressures indicate that at velocity ratios below 1.0 the boundary layer outside the ramp would have a tendency to flow away from the inlet. Second, it has been found that if the top edge of the diverging ramp walls were rounded, the effect of divergence would be greatly reduced. It was surmised that some of the improvement was caused by the resistance of the external boundary-layer air to flow over the rather sharp edge of the ramp walls.

Width-to-depth ratio.— The effect of varying the width-to-depth ratio of a submerged entrance is given in figure 11 for a constant ramp angle of 7° . Figure 11 shows that for the parallel wall, nondiverging ramp changing from a w/d ratio of 6 to a w/d ratio of 1 increases the maximum pressure recovery after diffusion from 70 to 80 percent. This trend was expected since most of the boundary-layer air in front of a nondiverging ramp flows into this type of entrance. Consequently, for the deeper and narrower entrances this low-energy air is a smaller percentage of the total quantity admitted. Increasing the divergence of the ramp walls diminished this effect. This was anticipated since, as mentioned previously, with a diverging ramp much of the boundary-layer air is diverted around the entrance, thus decreasing the beneficial effect of reducing the width-to-depth ratio found with a nondiverging ramp.

The width-to-depth ratio necessary for maximum pressure recovery also increased as the divergence increased. This may be better visualized by the following table:

	<u>Maximum Pressure Recovery (after Diffusion)</u>	<u>w/d for Maximum Recovery</u>	<u>V_1/V_0 for Maximum Recovery</u>
Parallel walls	0.80	1	0.70
Straight divergence No. 2	.845	2	.55
Straight divergence No. 3	.860	3	.43
Curved divergence	.865	3	.40

Since good pressure recoveries are obtained for diverging ramps over a wide range of inlet velocity ratios, this type of inlet should not be limited to systems which have small internal diffusion, but may include those which diffuse the air to a low velocity. It should be emphasized again that these pressure-recovery values are not the maximum obtainable but represent only those available with the existing boundary-layer thickness.

Ramp angle.— The results of varying ramp angle, given on figure 12, show that in all cases an increase in ramp angle was accompanied by a decrease in pressure recovery. As the divergence of the ramp plan form increased, this effect of the ramp angle became more pronounced.

An illustration of this, showing the pressure-recovery decrement between ramp angles of 5° and 11.5° for $w/d = 4$, is given as follows:

V_1/V_0	0.4	0.8	1.2
Nondiverging	0.055	0.03	0.045
Divergence No. 2	.04	.13	.15
Curved divergence	.12	.18	.19

The general trend of a decrease in pressure recovery resulting from an increase in ramp angle is also similar for w/d ratios of 2 and 6, the decrease being slightly less for $w/d = 2$ and greater for $w/d = 6$.

For entrances with nondiverging ramp walls this decrease in pressure recovery results from a thickening of the boundary layer due to a more adverse pressure gradient along the ramp. For the divergent ramp the problem is more complex for, instead of being relatively two-dimensional as it is for the nondiverging (parallel) walls, it assumes a three-dimensional aspect. In this case it is believed that much of the loss accompanying an increase in ramp angle is attributable to the resultant geometrical change in the ramp plan form. For a given divergent ramp, increasing the ramp angle increases the angle between the diverging walls. (See fig. 4.) This produces directly two adverse effects. First, increasing the angle between the ramp

~~SECRET~~

walls increases the tendency toward separation. Second, increasing this angle increases the obliquity between the ramp walls and the free-stream flow. This makes it more difficult for the air flowing along the outside edge to follow the divergent contour of the side walls. Consequently, air spills over the edge of the ramp walls, admitting much of the boundary layer and causing a cross flow between this air and the air flowing down the ramp. A combination of these two adverse conditions causes large pressure losses to occur in the corners of the submerged entrance when the ramp angle is increased. This is shown in figure 13, which gives the distribution of pressure loss across the submerged entrance for several configurations. From figure 12 it appears that for the larger ramp angles (above 10°) the optimum ramp plan form should have somewhat less divergence than that employed for the lower ramp angles.

From the results of the investigation of ramp angle, a better comparison of the merits of various width-to-depth ratios can be obtained. In most cases the use of a given ramp angle is dictated by the length available ahead of the duct entrance. For a constant-area duct entrance and a constant ramp angle, the required ramp length is much larger for the deep and narrow entrances. Thus for a 7° ramp angle, the ramp length for a w/d ratio of 1 is 2.45 times the ramp length of a w/d ratio of 6 entrance. Since ramp length usually constitutes a design limitation, a more usable comparison of the entrances of various width-to-depth ratios can be obtained by comparing the pressure recoveries at a constant ramp length. To obtain this comparison, pressure-recovery data after diffusion were plotted against a ramp-length term. This term was made nondimensional by squaring the ramp length and dividing by the duct entrance area. The cross plots of pressure recovery as a function of $\frac{(\text{ramp length})^2}{\text{entrance area}}$ are given in figure 14. A comparison of these curves indicates that for many design conditions width-to-depth ratios of 4 to 6 will give the highest pressure recovery.

Ramp-floor shape.— A comparison of the pressure recoveries for the straight and curved ramp floors is given in figure 15. The straight floor is seen to be superior for the configurations tested, but the difference in pressure recovery is small, usually less than 2 percent for the more optimum configurations. The present experimental results indicate this parameter to be of secondary importance in obtaining high-pressure recovery. Therefore, small changes in the contour of the floor that may be required to obtain a smooth junction between the ramp floor and fuselage skin should not noticeably affect the pressure

recovery of the installation.

Effect of boundary-layer thickness.— A comparison of the natural and thickened boundary layers is given in figure 16. Figure 17 shows that, as expected, increasing the boundary-layer thickness decreased the ram recovery. This decrease was practically the same for all configurations tested and was approximately equal to 0.12 ram recovery ratio. These tests clearly indicate that diverging the ramp walls keeps only a portion of the boundary-layer air from entering the duct, and consequently stresses the importance of locating the entrance in a region of thin boundary layer for maximum recovery.

An attempt was made to correlate the change in ram recovery with the change in boundary layer. Various boundary-layer parameters were considered (boundary layer, displacement, and momentum thicknesses, etc.) and the factor h was selected as being most pertinent in estimating the pressure recovery for this type of submerged inlet. The term h is defined as a height which contains an amount of free-stream ram pressure equivalent to the total pressure lost within the boundary layer, and may be evaluated from the following equation:

$$h = \int_0^{\delta} \frac{\Delta H}{H_0 - p_0} dy$$

where

δ total boundary-layer thickness

As a first approximation, the change in ram due to thickening the boundary layer or changing the duct depth and holding w/d constant, may be estimated from the following equation:

$$\Delta \left(\frac{H - p_0}{H_0 - p_0} \right) = \left(\frac{H - p_0}{H_0 - p_0} \right)_a - \left(\frac{H - p_0}{H_0 - p_0} \right)_b = \left(\frac{h}{B} \right)_a - \left(\frac{h}{B} \right)_b$$

where the subscripts a and b refer to different configurations. Obviously, this is not a rigorous relation, but it should give an indication of the change in ram which would be expected if the boundary-layer conditions of a given entrance were altered, or the size of the inlet changed (all dimensions remaining geometrically similar). The values of h for the natural boundary layer and the thickened boundary layer

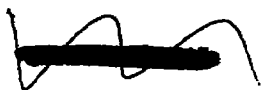
are 0.227 and 0.530 inch, respectively. A comparison of the estimated change in pressure recovery calculated by this equation with the measured change for the two boundary-layer conditions of these tests is given in the following table. This table is for ramps with curved divergence and a 7° ramp angle.

$\frac{V_1}{V_0}$	Calculated Values of $\Delta \left(\frac{H - P_0}{H_0 - P_0} \right)$			Measured Values of $\Delta \left(\frac{H - P_0}{H_0 - P_0} \right)$		
	$\frac{W}{d} = 2.0$	$\frac{W}{d} = 4.0$	$\frac{W}{d} = 6.0$	$\frac{W}{d} = 2.0$	$\frac{W}{d} = 4.0$	$\frac{W}{d} = 6.0$
0.4	0.071	0.101	0.123	0.095	0.120	0.112
0.8	.071	.101	.123	.105	.110	.113
1.2	.071	.101	.123	.095	.095	.105

The use of the h factor resulted in a much closer approximation than any of the other boundary-layer parameters considered.

Entrance Pressure Recovery.— Of primary interest in the design of a ducting system is the entrance pressure recovery, from which the losses chargeable to the diffuser are excluded. The method of computation used in determining this entrance pressure recovery is given in Appendix A.

The effects of ramp plan form, ramp angle and width-to-depth ratio, are shown in figures 18(a), (b), and (c). Comparison of these curves of entrance pressure recovery with corresponding curves for recovery after diffusion (figs. 10, 11, 12) show that the results follow the same trends. In general, the previous analysis accounting for the differences between various configurations is applicable. The slight discrepancies found in the analysis between data for entrance pressure recovery and pressure recovery after diffusion (figs. 11 and 12) can probably be attributed to changes in diffuser efficiency with changing entrance conditions. The losses at the entrance together with the losses after diffusion enable an evaluation to be made of the change in diffuser efficiency for any configuration. (See reference 2.) Using these losses, diffuser efficiencies for two entrance configurations have been calculated



and are compared in figure 19 with those obtained from bench tests. The difference between the two sets of curves represents the effect of the inlet on the diffuser efficiencies.

Pressure Distribution and Critical Mach Number

In this part of the investigation estimations of the critical-speed characteristics of the submerged duct entrances were made from an analysis of the pressure distributions over the lip and ramp. The critical Mach numbers were estimated from the peak low-speed pressure coefficients by the Kármán-Tsien method (reference 3). This method does not apply to three-dimensional flow (reference 4). Just what corrections should be used for the flow around a submerged inlet is not known, but it is believed the results given by the method of reference 3 will be conservative.

Lip.— The critical-speed characteristics of the lip are dependent upon the inclination of the flow approaching the lip. A decrease in the inclination of the flow is defined as an angular change of the flow which causes the stagnation point to move toward the outside surface of the lip. Thus, a decrease in the flow inclination decreases the incremental velocity over the outside surface of the lip, and vice versa for the inside surface.

The pressure distribution over the lip is given in figure 20. Here is shown the change in the stagnation point with inlet velocity ratio and the effect of this change on the peak negative pressure coefficients. Increasing the inlet velocity ratio always decreases the inclination of the flow.

The effects of ramp plan form on the critical-speed characteristics of the lip are given in figure 21(a). With a nondivergent ramp there is no appreciable change in the flow inclination across the entrance. For the lip section, 1 inch from the edge of the entrance, diverging the ramp also caused practically no variation from the data obtained with nondiverging walls. For the center-line section of the lip, however, diverging the ramp caused the stagnation point to move toward the outside and consequently increased the critical Mach number for the flow over the outside surface (fig. 21(a)). This comparison shows that with a divergent ramp there is a distinct variation across the entrance of the angle of flow approaching the lip. The flow near the edge of the entrance has a more positive inclination and produces the largest incremental velocities over the outside surface.

The effect of ramp angle on the critical Mach number for the lip is shown in figure 21(b). As would be anticipated, increasing



~~SECRET~~

the ramp angle decreased the flow inclination. The data verify that for the ramp angles tested there is a variation of the flow inclination across the entrance when a diverging ramp is used.

To correct for an undesirable angle of the flow approaching the lip, the incidence of the lip may be varied. The effect on critical Mach number of changing the lip incidence from -5° to $+5^\circ$ is shown on figure 22 for three width-to-depth-ratio entrances with curved divergence. From an analysis of these data, it appears that for many configurations the critical-speed characteristics of the lip will be improved by giving the lip a negative (down) incidence. The undesirable change in flow angle across the inlet, present with a divergent ramp, may also be compensated by giving the lip a more negative incidence near the edge of the entrance. Whether or not the lip incidence or camber should be varied across the entrance will depend on the critical speed of the airplane. It should be noted that it is undesirable to give the lip a more negative incidence than is required. Although the critical-speed characteristics may be improved at the lower inlet velocity ratios, the flow may separate from the inside surface at higher inlet velocity ratios, causing an added loss in pressure recovery.

Ramp.— The pressure-distribution data obtained along the ramp indicate that the inlet velocity ratio of the entrance does not affect the velocity from 40 percent of the ramp length to the start of the ramp (0-percent station, fig. 23(a)). The peak negative pressure coefficient occurs forward of the 40-percent station for inlet velocity ratios below 1.0, and, consequently, the critical-speed characteristics of the ramp appear to be independent of the inlet velocity ratio. The pressure distribution forward of the 40-percent station was found to be a function of the plan form of the ramp walls and the profile of the ramp floor.

The pressure distribution along the ramp is given in figure 23(b) for three ramp plan forms. The effect of width-to-depth ratio of the entrance and of ramp angle is given in figures 23(c) and 23(d), respectively. The critical Mach number for the ramp, as estimated from the pressure distribution, will be above 0.8 if the ramp angle does not exceed 9° .

The ramp floors for the aforementioned tests were all straight inclined surfaces. A comparison between the pressure distributions of the straight ramp floor and a curved ramp floor is given on figure 24. The pressure gradient over the straight ramp appears to be more favorable for both parallel and curved divergent ramp walls. The reduction in pressure recovery which accompanied the more adverse pressure gradient of the curved ramp floor has been mentioned previously. It may also be seen that the straight ramp floor gives

~~SECRET~~

lower peak incremental velocities over the ramp than the curved ramp floor when divergent walls are used. The studies of ramp floor contour in the present investigation were limited in scope. A more fundamental study of the effect of the ramp pressure gradient on critical speed and pressure recovery should be made. The ramp floor should probably be designed so that the pressure gradient will have the least slope at the design inlet velocity ratio.

Drag

Drag of the submerged entrances was determined by surveying the portion of the air stream containing the wake due to the inlet, and is equal to the difference in momentum of the air stream, with and without the duct installed. The method of calculating the drag is given in Appendix B. The drag coefficients based on duct-entrance area are presented in figure 25 for the various configurations, while figure 26 shows the distribution of the momentum loss aft of the entrance.

In all cases, the drag decreases as the inlet velocity ratio is increased. Figure 25(a) shows that the drag increases as the divergence is increased. This was expected, since a nondiverging ramp permits a larger portion of the boundary-layer air to flow into the inlet. In general, it appears that configurations which result in higher ram recovery have larger attendant drags. The negative values of drag result from the fact that the loss in momentum downstream of the entrance was less than the loss due to the boundary layer that previously existed. This can be seen on figure 26.

For the curved divergent ramp, the drag for most usable configurations should be quite low for the high-speed and climb flight range. Assuming a wing-area-to-duct-entrance-area ratio of 150, a typical C_D due to a submerged duct in the high-speed attitude would be approximately from 0.0003 to 0.0006. It should be remembered that the effect of the duct wake along the fuselage aft of the entrance is not included.

Deflectors

Deflectors, or ridges along the divergent contour of the entrance, have been shown to increase the ram recovery when used with certain inlet configurations and conditions. This series of tests was performed to find the effect of deflector size, and to evaluate the use of deflectors for various inlet configurations. The criteria used for evaluation were the same as those for the principal investigation.

It was found that increasing the deflector length from 25 to 50 percent of the ramp length caused the most pronounced increase in pressure recovery (fig. 27(a)), except for the 0.25-inch-high deflectors. Further increases to 100 percent of the ramp length caused increases in the ram recovery only at inlet velocity ratios below about 0.8. Figure 27(b) also gives the pressure recoveries for deflector heights of 0.25, 0.50, 0.75, and 1.00 inch when tested at various lengths.

For the deflector heights tested it may be said, in general, that increasing the height increased the pressure recovery, particularly at inlet velocity ratios above 0.5. However, changing the height from 0.75 to 1.00 inch improved the recovery only at inlet velocity ratios above 1.0. As a result of these tests on deflector size, a series of deflectors was selected for further investigation. Deflector heights ranging from 0.25 to 0.75 inch extending 50 and 100 percent of the ramp length were chosen because it was thought that this range was most practicable.

The change in ram recovery produced by deflectors for three width-to-depth ratios can be obtained from figure 28. The data show that using deflectors with the more shallow entrances (w/d ratios of 4.0 and 6.0) adds a larger increment to the pressure recovery. This can be better visualized by the following table which lists the increase in pressure recovery after diffusion resulting from the use of deflectors. The data are for a 7° curved divergent ramp and the deflectors are 0.75 inch high and 100 percent of the ramp length.

$\frac{V_1}{V_0}$	$\frac{w}{d} = 2.0$	4.0	6.0
0.5	0.019	0.046	0.076
.7	.084	.103	.120
1.0	.088	.123	.138

Figure 28 also shows that changing the deflector length from 50- to 100-percent ramp length causes little effect on the ram recovery of the entrance with $w/d = 2$.

Figure 29(a) shows the difference in ram recovery for various ramp plan forms with and without deflectors. It is apparent that

deflectors are not equally beneficial for all ramps. The increment of ram recovery due to deflectors increased with increasing divergence. With nondivergent (parallel) walls the improvement was negligible.

The results of tests to find the effect of deflectors on ramp angle are shown in figure 29(b). When these data are compared with those for similar configurations without deflectors (fig. 12) it can be seen that deflectors are beneficial, from the standpoint of ram recovery, for all installations. A more comprehensive comparison of the three w/d ratios tested can be obtained from the cross plots of these data, given in figure 30. Here is shown the pressure recovery as a function of the ramp-length term previously derived.

Pressure recovery at the duct entrance is given in figure 31 for several deflector-entrance configurations. The trends shown by these data are in good agreement with the analysis already discussed.

Deflectors apparently increase the pressure recovery by assisting the air flowing outside the ramp to follow the diverging contour of the side walls. This prevents much of the cross flow of air over the top edge of the ramp walls and also helps to divert more of the boundary layer around the entrance. With regard to the selection of a deflector to give best recovery, it should be noted that results of other investigations (reference 2) clearly indicated that the requirements for deflectors are dependent upon the location of the entrance. It was found that when the entrance was placed in a region of thin boundary layer, increasing the deflector length from 50- to 100-percent ramp length caused a definite decrease of pressure recovery. It is probable that deflectors which extend the full length of the ramp should be used only for thick boundary-layer conditions.

Although the use of deflectors results in higher pressure recovery, it was found that their effect was somewhat deteriorating to drag characteristics of the entrance. Figure 32 gives the drag for several inlet configurations with deflectors. Comparing these data with drag for similar configurations without deflectors (fig. 25) shows that deflectors increased the drag for all configurations tested when the air enters the inlet at a velocity ratio above 0.6. This comparison also indicates the deflectors caused the largest drag for shallow entrances ($w/d = 4.0$ and 6.0) and steep ramp angles where the gain in pressure recovery was the greatest. As would be expected, figure 32(c) also shows that increasing the deflector size, both length and height, increased the drag.

The pressure distribution over the ramp when deflectors are used is given in figure 33. Comparison of these data with figure 23 indicates that deflectors cause some addition to the incremental velocities over the ramp. The critical-speed characteristics of the lip for the curved diverging ramp, with and without deflectors,

are given in figure 34. This comparison shows that deflectors increase the critical Mach number for the flow over the outside surface at the center section of the entrance while decreasing the MCR for this flow near the edge of the entrance. A larger flow-angle variation across the entrance is therefore indicated when deflectors are used.

POSSIBLE APPLICATIONS FOR NACA SUBMERGED INLETS

It should not be maintained that the submerged entrance is applicable as an inlet for all ducting installations, but it does have certain characteristics in addition to those presented which make it particularly suited for specific ducting applications. The use of NACA submerged inlets could, in some cases, result in greater aerodynamical cleanness by effecting more favorable fuselage contour lines and perhaps reducing the fuselage frontal area. The structural complexity of the ducting system should be diminished and larger space provided for internal components. This type of duct should also reduce considerably the ingestion of foreign material by inertia separation.

A possible jet-engine installation utilizing NACA submerged ducts is shown in figure 35. In this illustration the submerged-duct design is centered around a single jet engine located in the fuselage aft of the pilot's enclosure. Placement of the twin entries ahead of the wing minimized the influence of the wings pressure field and situated the entry in a region of thin boundary layer (reference 2). A w/d ratio of about 4 seemed advisable from internal space limitations, and a ramp using curved divergence together with a ramp angle between 5° or 7° was selected. This installation should give optimum pressure recovery, low over-all drag and an efficient internal-flow system, since the necessity for sharp bends and rapid expansions have been eliminated. Reference 2 discusses a duct-flow instability that could occur with this type of installation.

For airplanes employing two jet engines the necessity of using wing nacelles could often be eliminated by housing the engines side by side in the fuselage. The NACA submerged inlet appears to be very adaptable to such an installation. The use of single ducts leading to each jet engine would be similar in design and location to that shown in the previous illustration. With a single duct leading to one jet engine, the flow instability previously mentioned could not occur. The short internal ducting of such an installation should result in minimum losses, especially for engines with axial-type compressors.

Certain types of missiles, which are powered by jet engines in

the fuselage and have no provision for landing gear, are ideally adaptable for an NACA submerged-duct system. The single inlet could be placed on the underside of the fuselage and the installation would have the design and aerodynamic advantage mentioned previously.

Other applications could include some ducting systems involving cooling and carburetor air. If this type of entrance could be substituted for the protruding scoop-type of inlet, the aerodynamic neatness of the aircraft would be greatly enhanced.

CONCLUSIONS

From investigations that have been made of the configuration changes and parameters affecting the design of NACA submerged-duct installations it was concluded that:

1. The boundary layer at the location of the submerged entrance will influence the ram recovery. Due to the relatively thick tunnel boundary layer into which the entrance was placed, it is believed that the pressure recoveries presented in this report are lower than could be expected for most airplane installations but that the comparison between configurations is valid.
2. Significant gains in pressure recovery for a wide range of configurations resulted from the use of the curved divergent ramp. This is especially true in the low inlet-velocity-ratio range, $\frac{V_1}{V_0} \leq 0.9$, where high pressure recovery is most necessary.
3. The effect of width-to-depth ratio was greatest for the nondivergent (parallel) ramp walls. The best recovery for this configuration occurred for a w/d ratio = 1 (square) entrance. As the ramp-wall divergence increases w/d ratio has less effect, and the square entry is inferior to most rectangular entries. With curved divergence the ram recovery increment due to change in w/d ratio is about half that with parallel walls.
4. Ramp angle or, in some cases, ramp length, had an outstanding effect on ram recovery. The detrimental effect of increasing ramp angle became greater as the divergence was increased.
5. In general, it appears that an inlet with curved divergence, a 5° or 7° ramp angle, and a w/d ratio of from 3 and 5 offers optimum characteristics.
6. Good critical-speed characteristics can be obtained with proper lip design. There is a spanwise change in angle of attack of the lip when a diverging ramp is used, and it may be necessary to

twist the lip, depending on the pressure field into which the entrance is placed.

7. For most design conditions the drag was found to be small. However, in the selection of an optimum configuration, the drag and ram recovery should be weighed. In this respect, the use of deflectors may not always prove advantageous.

Ames Aeronautical Laboratory,
National Advisory Committee for Aeronautics,
Moffett Field, Calif.

APPENDIX A

METHOD OF OBTAINING DUCT LOSSES AT THE ENTRANCE

AND AFT OF THE DIFFUSER SECTION

If, as in the most general case, the stream filaments for a steady flow are not assumed to have the same flow energy, then the total pressure for a given weight of fluid passing a given section is (reference 5)

$$H = \frac{1}{\rho_{\text{mean}} V_{\text{mean}} A} \int H_{\text{local}} \rho_{\text{local}} V_{\text{local}} dA \quad (\text{A1})$$

Usually, it is not necessary to apply this exact method, but it may be requisite if the total pressure distribution at the measuring station has local regions of high loss. Such was the case at the submerged-duct entrance for inlet velocity ratios between 0 and 0.8. In computing the losses for this range, equation (1) was modified to reduce the computational work:

$$H = \frac{1}{\rho_{\text{mean}} V_{\text{mean}} A} \sum_{n=1}^{n=l} h_n \rho_n V_n a_n \quad (\text{A2})$$

where

- ~~_____~~
 h local total head
 ρ local density
 a local area
 V local velocity
 l number of equal areas (equals number of tubes)

assuming

$$\rho_{\text{mean}} = \rho_n = \rho_1 = \rho_2 = \text{etc.}$$

$$a_1 = a_2 = a_3$$

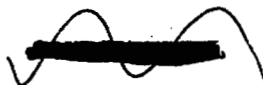
$$A = a \times l$$

Then

$$H = \frac{1}{l} \sum_{n=1}^{n=l} h_n \frac{V_n}{V_{\text{mean}}} + h_2 \frac{V_2}{V_{\text{mean}}} \dots h_m \frac{V_m}{V_{\text{mean}}} \quad (\text{A3})$$

For this application subscripts 1, 2, etc., denote local areas considered.

The difference between the losses computed in the preceding manner and those obtained from an integrating manometer were found to be negligible at the entrance for the remainder of the inlet-velocity-ratio range, V_1/V_0 's from 0.8 to 1.4. Such was the case also for the entire inlet-velocity-ratio range at the measuring station after diffusion.



~~SECRET~~

APPENDIX B

METHOD OF OBTAINING DRAG OF THE SUBMERGED ENTRANCES

If the momentum change between two stations along a stream tube is measured, the resulting drag force may be computed:

$$D = \int (U - u) dm \quad (B1)$$

or

$$D = \rho \int u(U_0 - u) dA \quad (B2)$$

where one station is in the free stream.

Assuming the densities at U_0 and u are equal,

$$C_{DD} = \frac{D}{A q_0} = \frac{2}{A} \int \frac{u}{U_0} \left(1 - \frac{u}{U_0} \right) dA \quad (B3)$$

Now, assuming that free-stream static pressure exists in the wake ($p = p_0$)

Then

$$C_{DD} = \frac{2}{A} \iint \sqrt{1 - \frac{\Delta H}{q_0}} \left(1 - \sqrt{1 - \frac{\Delta H}{q_0}} \right) dy dx \quad (B4)$$

or

$$C_{DD} = \frac{2}{A} \iint \left(1 - \frac{\Delta H}{q_0} \right)^{\frac{3}{2}} dy dx - \frac{2}{A} \iint dy dx + \frac{2}{A} \iint \frac{\Delta H}{q_0} dy dx \quad (B5)$$

~~SECRET~~

Expanding the first part of this equation in a binomial expansion and combining with the remainder gives

$$C_{DD} = \frac{1}{A} \iint \frac{\Delta H}{q_0} dy dx - \frac{1}{4A} \iint \left(\frac{\Delta H}{q_0} \right)^2 dy dx \dots \quad (B6)$$

It was found that there were sufficient tubes in the measuring rake so that a value of $\frac{\Delta H}{q_0}$ obtained with the aid of an integrating manometer and substituted in place of the integrals in equation (B6) gave very satisfactory correlation with the point-by-point integration of equation (B4).

To indicate how the submerged-duct-drag determination was made, it might be best to consider a comparison between the drag of a nose inlet and of a submerged inlet as determined by momentum surveys. This comparison should include the air flow through the entrance to corresponding stations at the jet-engine compressor. What happens after this section is a function of the jet-engine characteristics and does not enter this discussion. To simulate the preceding condition, consider that the air after entering the duct is removed at right angles to the air stream so that there is no momentum of the exit air in the drag direction. Then

	Loss in momen- tum of the	Momentum of		Loss in momentum
Drag of inlet =	entering air at	+ entering air +	+	behind the duct
	the duct entrance	(ram drag)		(profile drag)

For the nose inlet

$$D = 0 + \frac{m_{ent}}{M_{ent}} V_0 + \int m_{aft} (V_0 - V_{aft}) dA_{aft}$$

For the submerged inlet

$$D = \int m_{ent} (V_0 - V_{ent}) dA_{ent} + \int m_{ent} V_{ent} dA_{ent} + \int m_{aft} (V_0 - V_{aft}) dA_{aft}$$

where m is the mass flowing through each unit area.

Usually, for the nose-type inlet, the momentum of the entering air is taken into account as part of the internal drag and subtracted out. To make a fair comparison between the nose and submerged inlets, for a given quantity of flow, the same ram drag should be accounted for in each case. However, for this condition, the ram drag of the submerged entrance is less than that for the nose inlet since air is inducted which has already received a loss of momentum, this loss being equal to the second term of the previous equation. If it is assumed that the momentum of the entering air is $(m_{ent}V_o)$ for both installations and is subtracted from each case, the drag becomes:

For the nose inlet

$$D = \int m_{aft}(V_o - V_{aft}) dA_{aft}$$

For the submerged inlet

$$D = \int m_{aft}(V_o - V_{aft}) dA_{aft}$$

In an actual duct application, the air flow over the body with the duct entrance removed must be considered, so that another term is necessary. The final form of the equation used to evaluate the drag then becomes:

$$D = \int m_{aft}(V_o - V_{aft_{duct\ in}}) dA_{aft} - \int m_{aft}(V_o - V_{aft_{duct\ out}}) dA_{aft}$$


REFERENCES

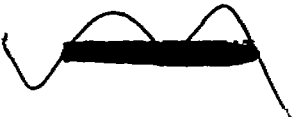
1. Frick, Charles W., Davis, Wallace F., Randall, Lauros M., and Mossman, Emmet A.: An Experimental Investigation of NACA Submerged-Duct Entrances. NACA ACR No. 5I20, 1945.
 2. Mossman, Emmet A., and Gault, Donald E.: Development of NACA Submerged Inlets and a Comparison with Leading-Edge Inlets for a 1/4-Scale Model of a Fighter Airplane. NACA CRM No. A7A31, 1947.
 3. von Kármán, Th.: Compressibility Effects in Aerodynamics. Jour. Aero. Sci., vol. 8, no. 9, July 1941, pp. 337-356.
 4. Lees, Lester: A Discussion of the Application of the Prandtl-Glauert Method to Subsonic Compressible Flow over a Slender Body of Revolution. NACA TN No. 1127, 1946.
 5. Rouse, Hunter: Fluid Mechanics for Hydraulic Engineers. McGraw-Hill, 1938, pp. 47-54.
- 

TABLE I

Index of the Submerged-Duct-Entry Modifications

	Ramp plan form	w/d	Ramp angle	Ramp floor shape	Boundary thickness	Deflectors
Ramp plan form	Parallel walls Straight divergence No. 2 Straight divergence No. 3 Curved divergence	4, 6	7°	Straight	Natural	None
w/d	Parallel walls Straight divergence No. 2 Straight divergence No. 3 Curved divergence	1, 2, 3, 4, 5, 6	7°	Straight	Natural	None
Ramp angle	Parallel walls Straight divergence No. 2 Curved divergence	2, 4, 6	a. 5°, 7°, 9°, 11.5°, b. 15°	Straight	Natural	None
Ramp floor shape	Parallel walls Curved divergence	4	c. 5°, 7°, 9°, 11.5°	Curved	Natural	None
Boundary thickness	Curved divergence	2, 4, 6	7°	Straight	Thickened	None
Deflectors ^d	Parallel walls Straight divergence No. 2 Curved divergence	2, 4, 6	5°, 7°, 9° 11.5°, 15°	Straight	Natural	Height = 1/4 in., 1/2 in., 3/4 in., 1 in. Length = 25%, 50%, 75%, 100%

a. Only with w/d = 4 and 6.

b. Only with w/d = 2.

c. Angle defined by a straight line connecting beginning and end of ramp.

d. See table II for combinations tested.

TABLE II

RANGE OF DEFLECTOR TESTS

Height		1/4 inch	1/2 inch	3/4 inch	1 inch
Length					
25%	w/d	4	--	4	--
	Ramp angle	7°	--	7°	--
50%	w/d	4	4	4	4
	Ramp angle	7°	7°	7°	7°
75%	w/d	4	4	4	4
	Ramp angle	7°	7°	7°	7°
100%	w/d	2, 4, 6	4	2, 4, 6	4
	Ramp angle	7°	7°	5°, 7°, 9°, 11.5°, 15°	7°

NATIONAL ADVISORY
COMMITTEE FOR AERONAUTICS

TABLE III

FIGURE GUIDE TO RESULTS

Modification	Pressure recovery	Pressure distribution	Drag
Ramp plan form	Figs. 10, 18	Figs. 21, 23	Figs. 25, 26
w/d	Figs. 11, 18	Figs. 22, 23	Figs. 25, 26
Ramp angle	Figs. 12, 13, 14, 18	Figs. 21, 23	Figs. 25, 26
Ramp floor shape	Fig. 15	Fig. 24	None
Boundary-layer thickness	Fig. 17	None	None
Deflectors	Figs. 27, 28, 29, 30, 31	Figs. 33, 34	Fig. 32

NATIONAL ADVISORY
COMMITTEE FOR AERONAUTICS

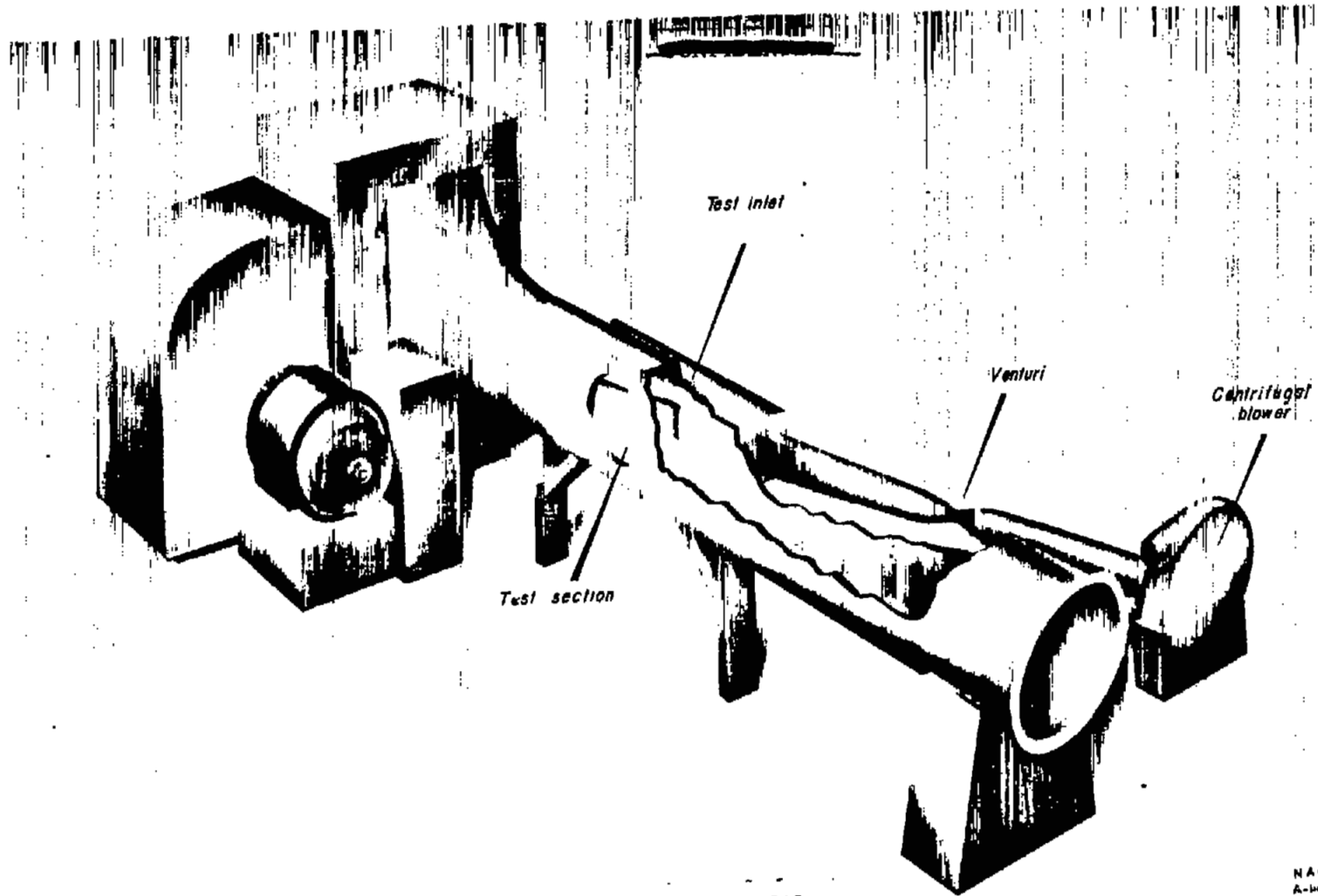
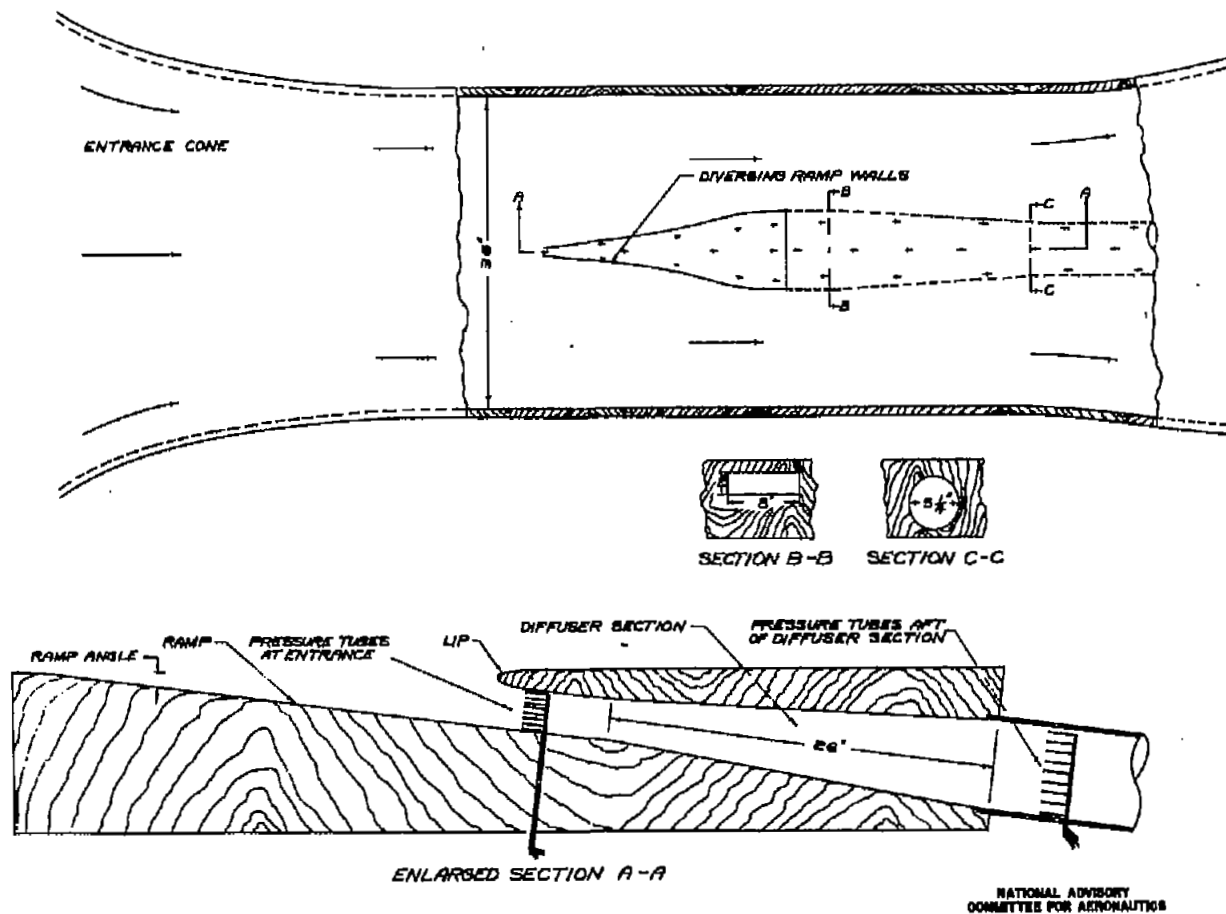


Figure 1.- Schematic view of the 8- by 36-inch wind tunnel.

NACA
A-148.
7-18-47



NATIONAL ADVISORY
COMMITTEE FOR AERONAUTICS

FIGURE 2. -THE GENERAL ARRANGEMENT OF A SUBMERGED DUCT ENTRANCE MODEL TESTED IN THE 8-BY 36-INCH WIND TUNNEL.

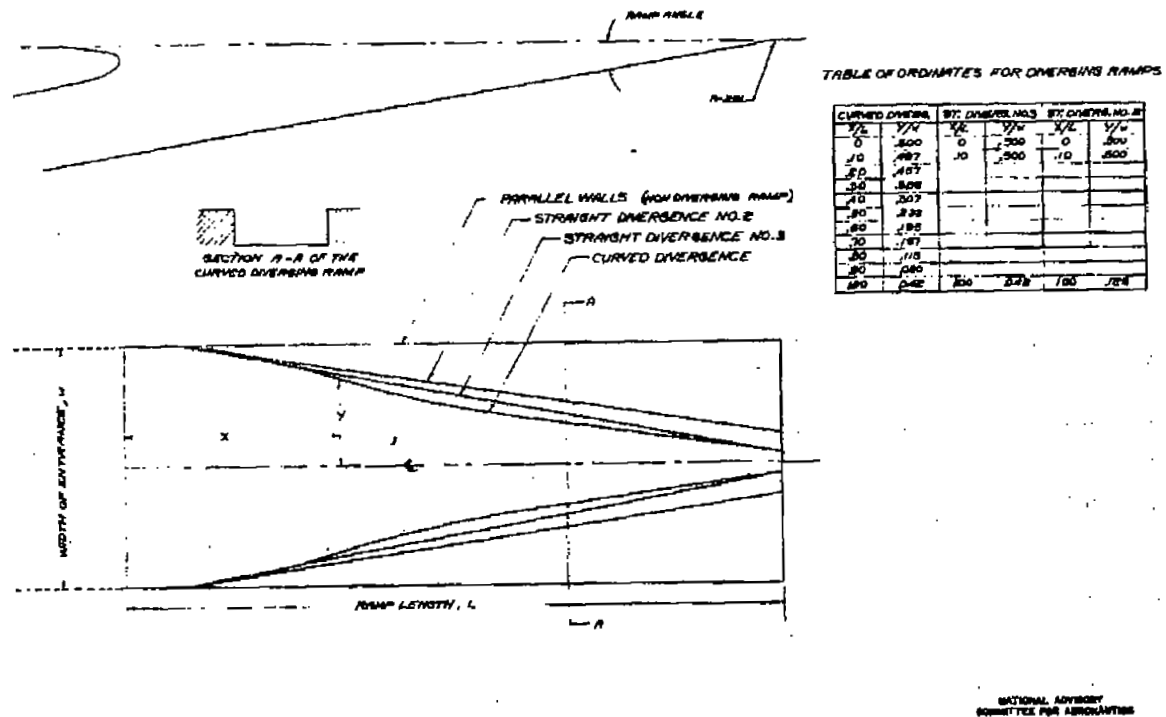
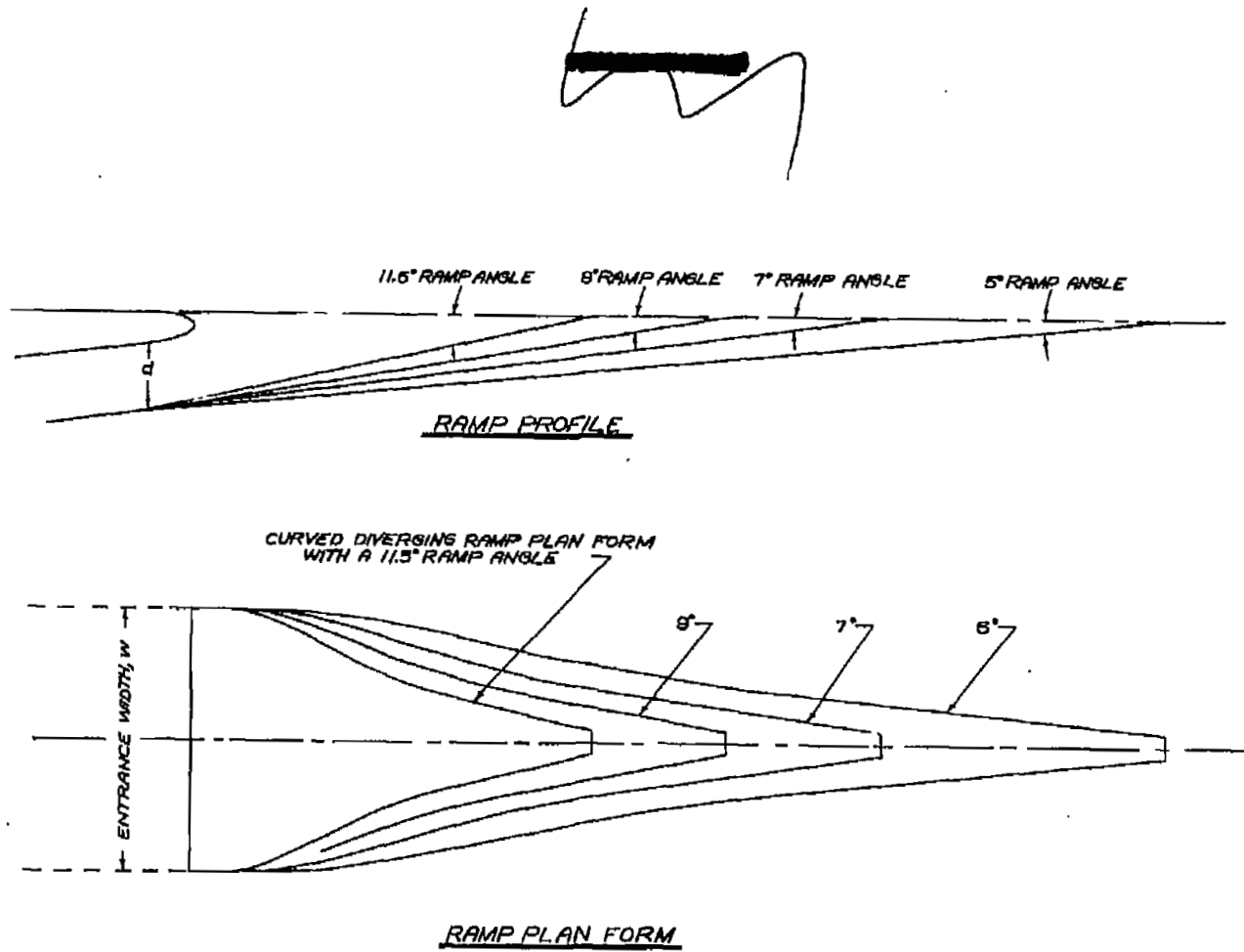


FIGURE 3. - FOUR PLAN FORMS OF THE RAMP TESTED IN THIS INVESTIGATION OF THE SUBMERGED DUCT ENTRANCES



NATIONAL ADVISORY
COMMITTEE FOR AERONAUTICS

FIGURE 4.— THE GEOMETRIC CHANGE OF THE RAMP WITH RAMP ANGLE; CURVED DIVERGENCE, $w/d = 4.0$.

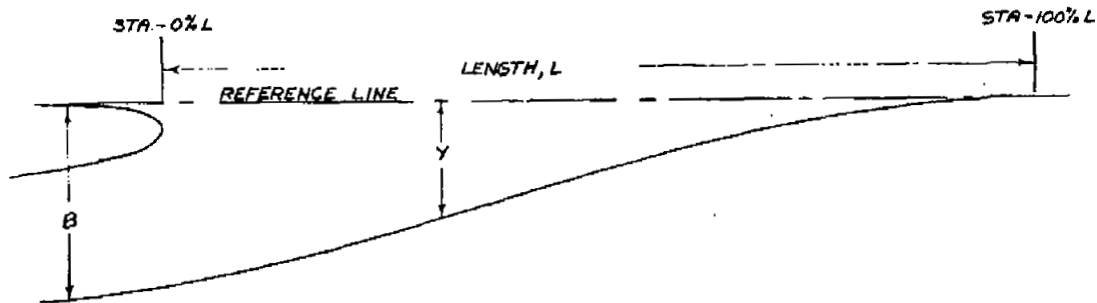


TABLE OF ORDINATES

NOTE

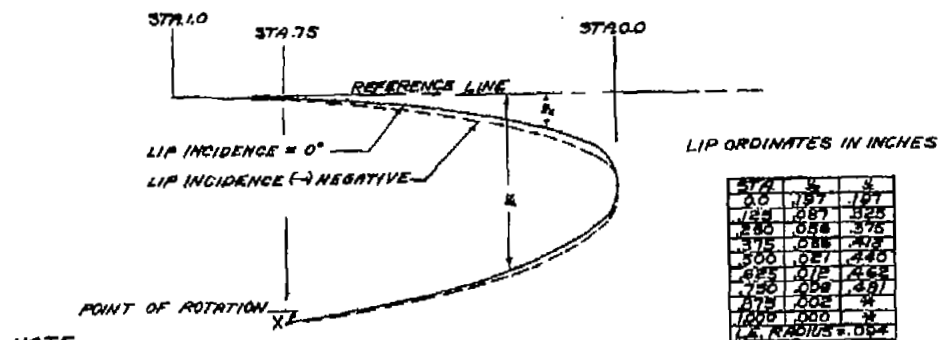
L = LENGTH BETWEEN START OF RAMP AND STATION AT WHICH THE DEPTH OF THE DUCT ENTRANCE IS MEASURED

B = DISTANCE FROM REFERENCE LINE TO RAMP @ -5.64% L STATION. (POINT AT WHICH DUCT ENTRANCE AREA IS MEASURED)

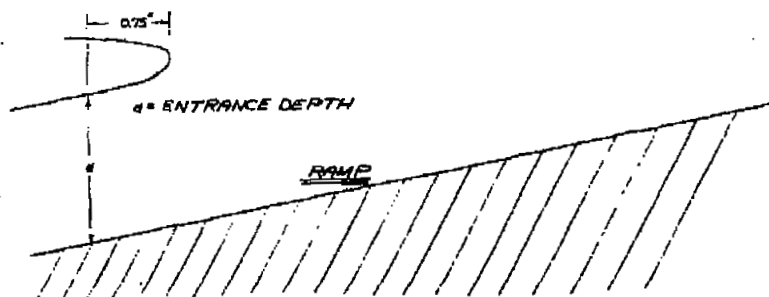
STA-%L	Y-%B
100.00	0.00
91.78	0.40
83.40	4.05
75.00	10.15
66.68	18.10
58.33	29.36
50.04	41.09
41.68	53.20
33.34	65.48
25.02	77.20
16.67	87.62
8.34	95.70
0.00	100.0

NATIONAL ADVISORY
COMMITTEE FOR AERONAUTICS

FIGURE 5. - THE CURVED RAMP FLOOR TESTED IN THIS INVESTIGATION OF THE SUBMERGED DUCT ENTRANCES.



- NOTE
1. ALL DIMENSIONS AND ORDINATES ARE FOR A SUBMERGED ENTRANCE OF 1.0 INCH DEPTH
 2. TO OBTAIN LIP FOR A SPECIFIC ENTRANCE MULTIPLY THE ORDINATES GIVEN IN THIS FIGURE BY THE ENTRANCE DEPTH IN INCHES



NATIONAL ADVISORY
COMMITTEE FOR AERONAUTICS

FIGURE 7.- THE LIP PROFILE USED IN THIS INVESTIGATION OF THE SUBMERGED ENTRANCE.

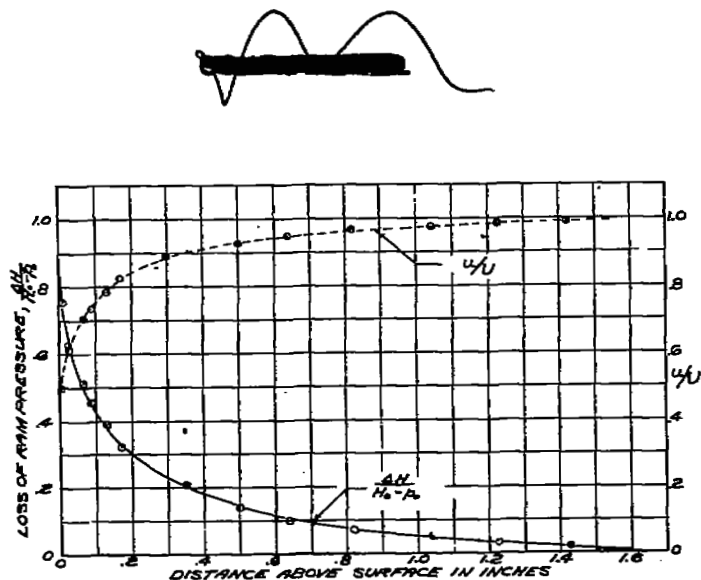
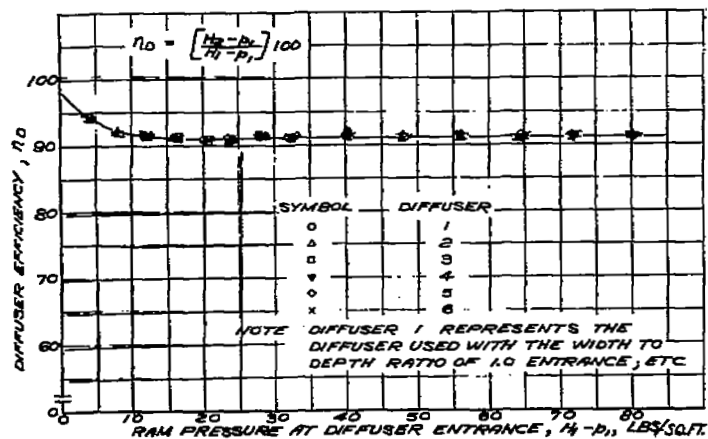
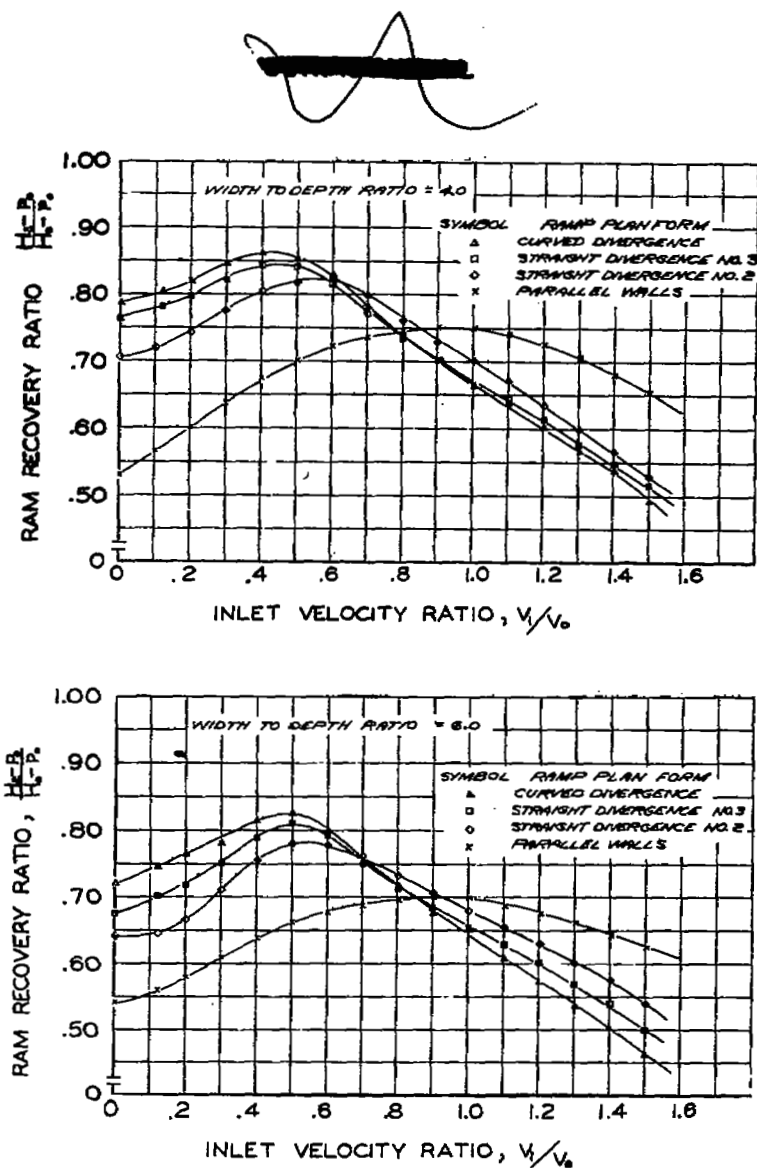


FIGURE 8.- THE NATURAL BOUNDARY LAYER OF THE WIND TUNNEL WALL MEASURED AT THE LOCATION OF THE DUCT ENTRANCE.



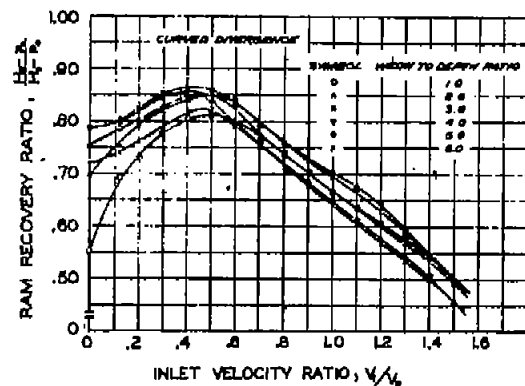
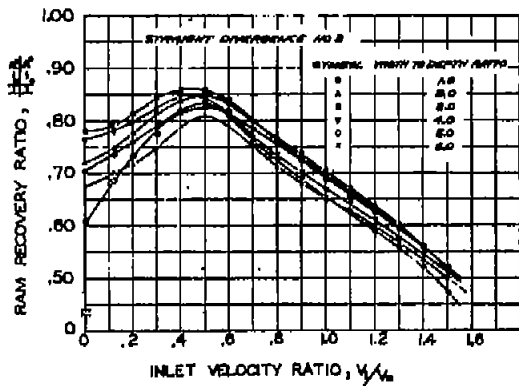
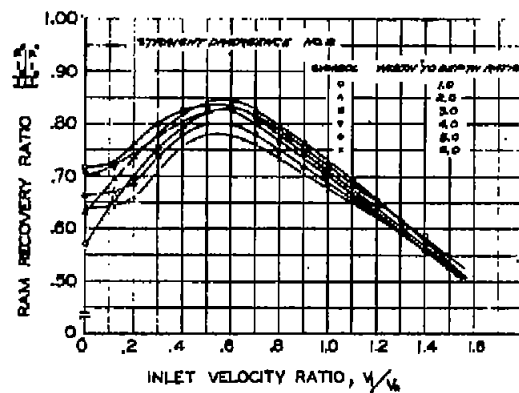
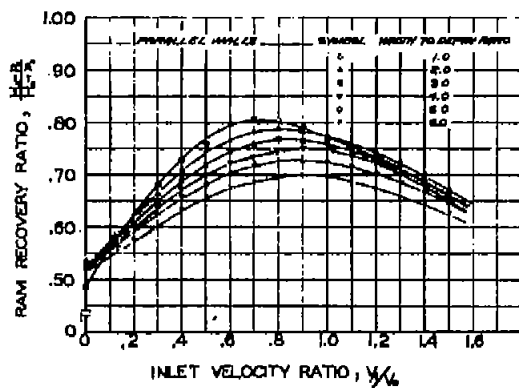
NATIONAL ADVISORY
COMMITTEE FOR AERONAUTICS

FIGURE 9.- THE EFFICIENCIES OF THE DIFFUSER SECTIONS USED WITH THE VARIOUS MODELS OF THE SUBMERGED ENTRANCE.



NATIONAL ADVISORY
COMMITTEE FOR AERONAUTICS

FIGURE 10.- VARIATION OF RAM RECOVERY RATIO, MEASURED AFTER THE DIFFUSER SECTION, WITH INLET VELOCITY RATIO FOR FOUR PLAN FORMS OF THE RAMP. 7° RAMP ANGLE.



NATIONAL ADVISORY
COMMITTEE FOR AERONAUTICS

FIGURE 11. - VARIATION OF RAM RECOVERY RATIO, MEASURED AFTER THE DIFFUSER SECTION, WITH INLET VELOCITY RATIO FOR FOUR RAMP PLAN FORMS AND SIX WIDTH TO DEPTH RATIOS OF THE ENTRANCE. γ RAMP ANGLE

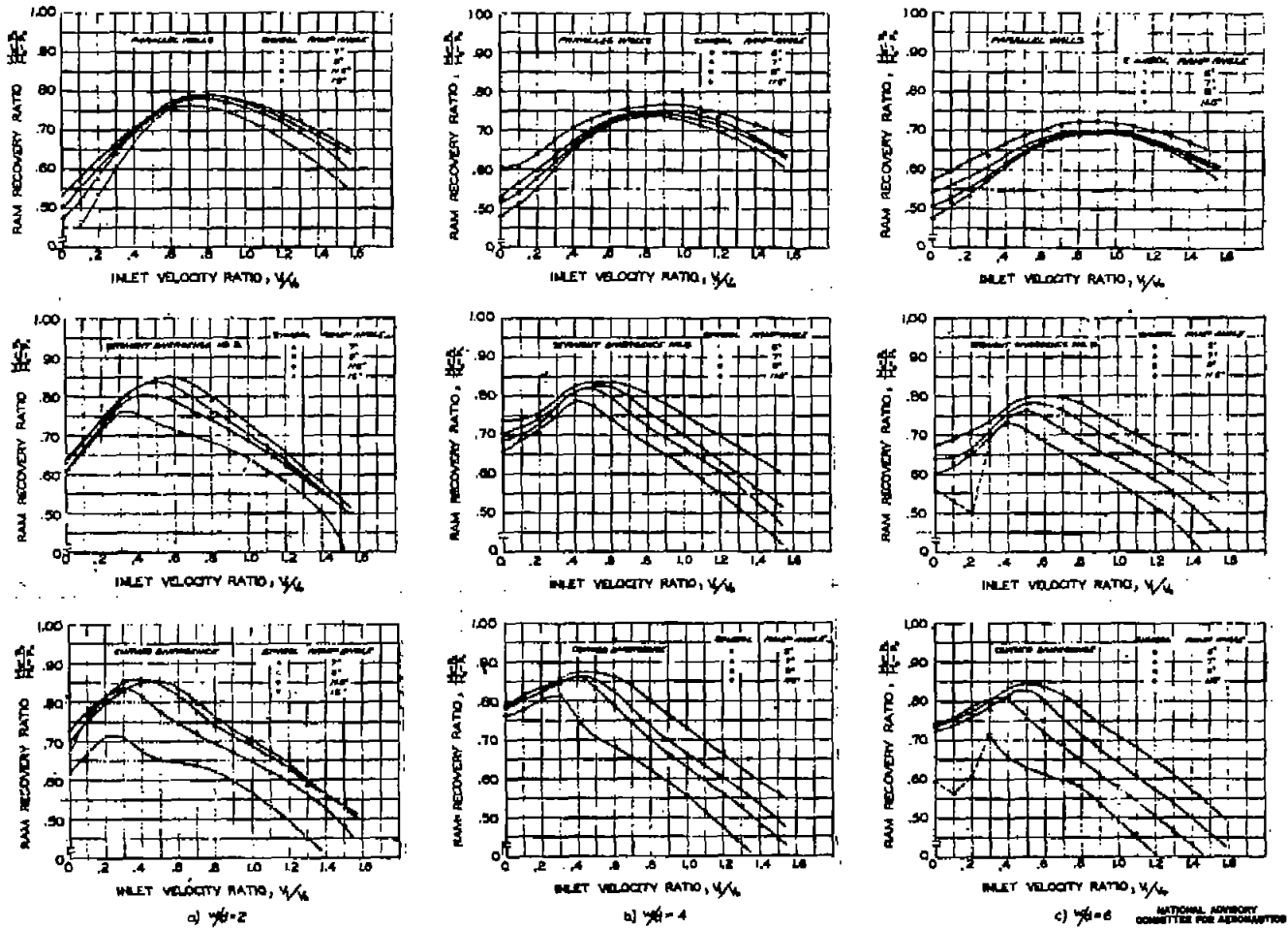


FIGURE 12.-THE EFFECT OF RAMP ANGLE ON THE VARIATION OF RAM RECOVERY RATIO, MEASURED AFTER THE DIFFUSER SECTION, WITH INLET VELOCITY RATIO FOR SEVERAL ENTRANCE CONFIGURATIONS.

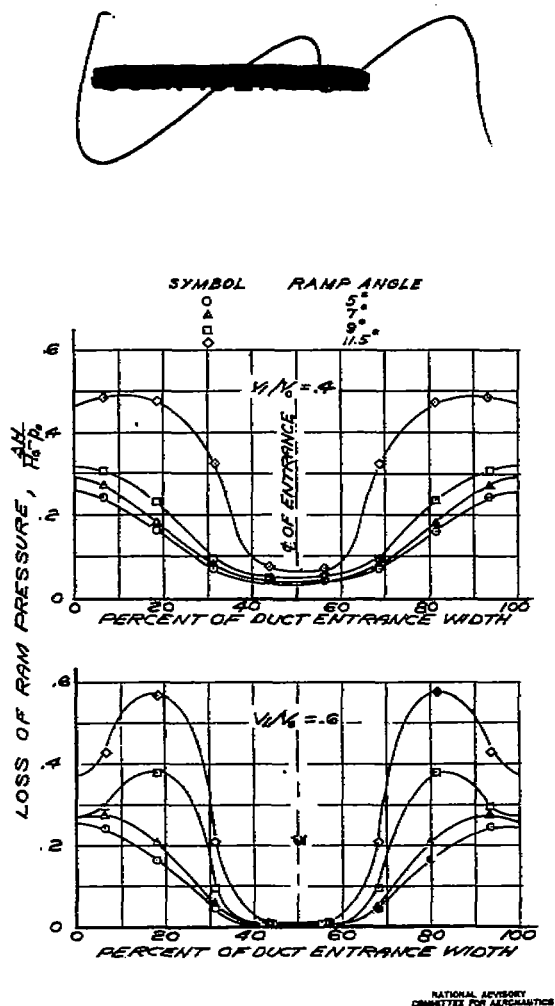


FIGURE 13. - DISTRIBUTION OF THE LOSS OF RAM PRESSURE ACROSS THE SUBMERGED ENTRANCE FOR VARIOUS RAMP ANGLES. $V_1/V_0 = 4$; CURVED DIVERGENCE.

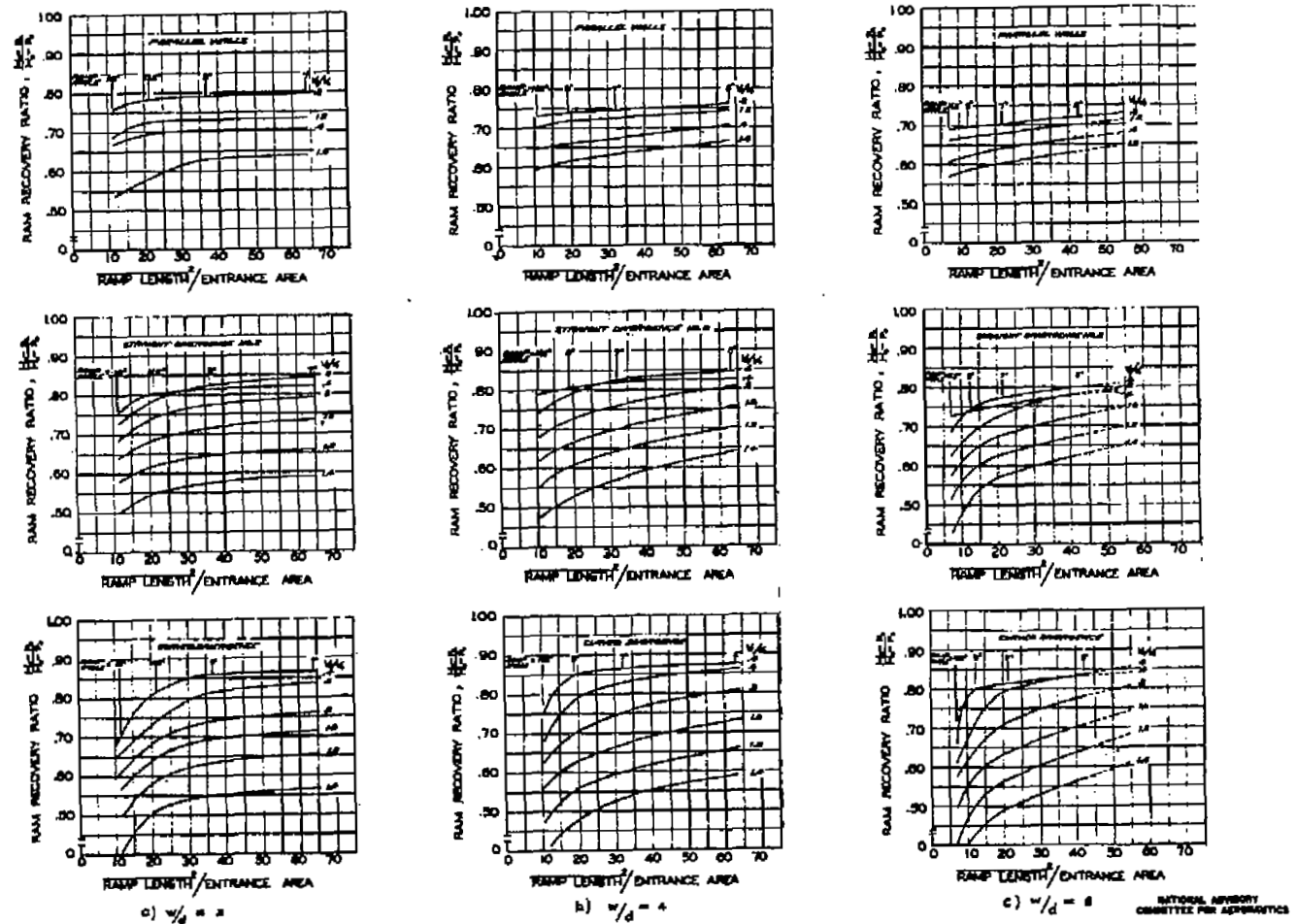
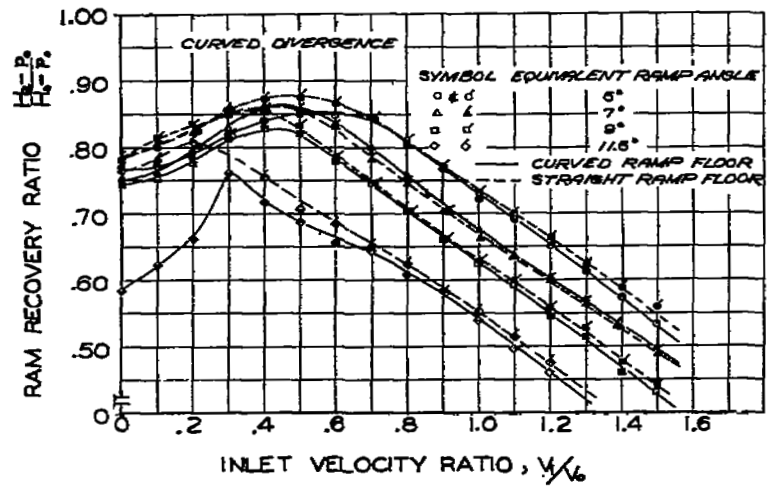
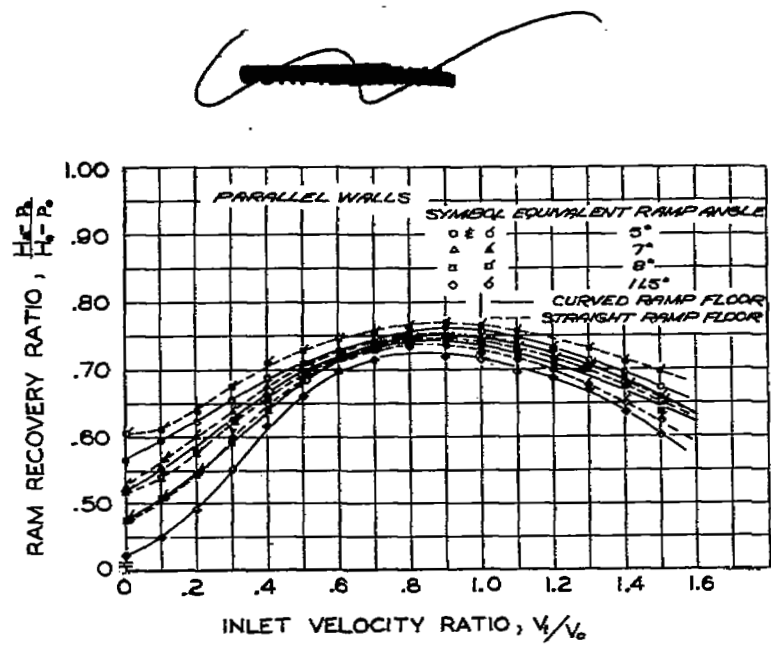


FIGURE 14 - VARIATION OF RAM RECOVERY RATIO, MEASURED AFTER THE DIFFUSER SECTION, WITH RAMP LENGTH COEFFICIENT FOR VARIOUS ENTRANCE CONFIGURATIONS.



NATIONAL ADVISORY
 COMMITTEE FOR AERONAUTICS

FIGURE 15.—THE EFFECT OF RAMP FLOOR SHAPE ON RAM RECOVERY MEASURED AFTER THE DIFFUSER SECTION. $\gamma/H = 4$

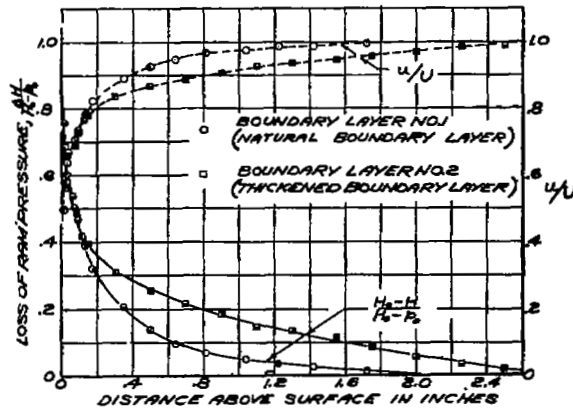
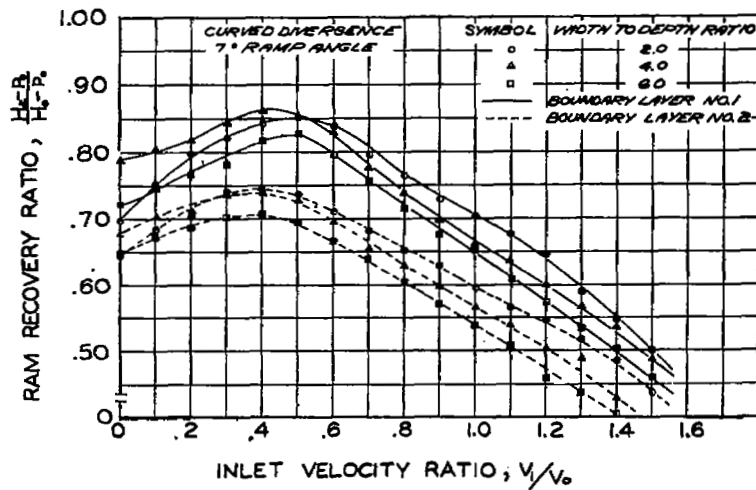


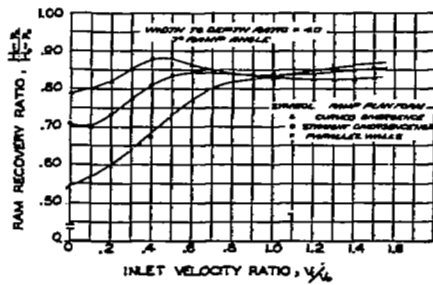
FIGURE 16.- COMPARISON OF THE TWO BOUNDARY LAYERS OF THE WIND TUNNEL WALL, MEASURED AT THE LOCATION OF THE DUCT ENTRANCES.



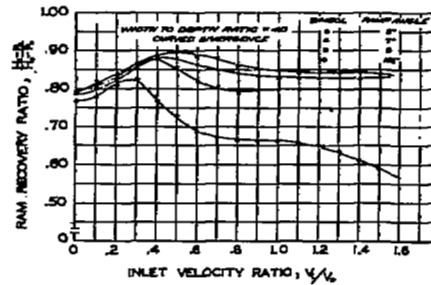
NATIONAL ADVISORY COMMITTEE FOR AERONAUTICS

FIGURE 17.- COMPARISON OF RAM RECOVERY, MEASURED AFTER THE DIFFUSER SECTION, FOR THE TWO BOUNDARY LAYER CONDITIONS, CURVED DIVERGENCE.

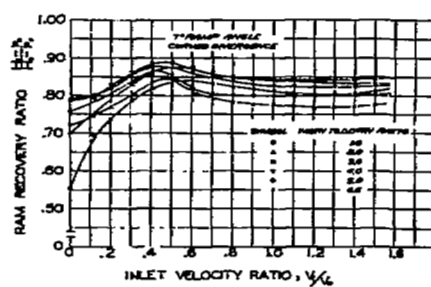
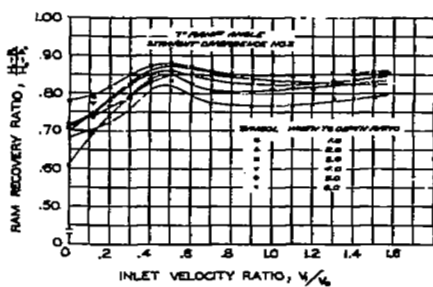
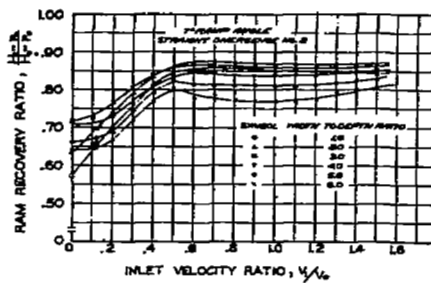
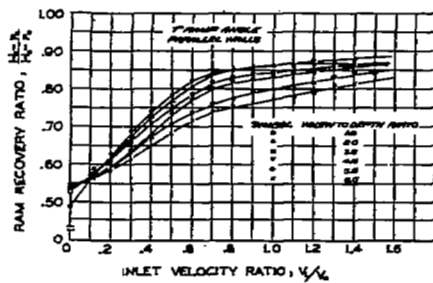
CONFIDENTIAL



(a) EFFECT OF RAMP PLAN FORM



(b) EFFECT OF RAMP ANGLE



(c) EFFECT OF THE WIDTH TO DEPTH RATIO OF THE ENTRANCE

NATIONAL ADVISORY
COMMITTEE FOR AERONAUTICS

FIGURE 18.- VARIATION OF RAM RECOVERY RATIO, MEASURED AT THE SUBMERGED ENTRANCE, WITH INLET VELOCITY RATIO FOR VARIOUS INLET CONFIGURATION.

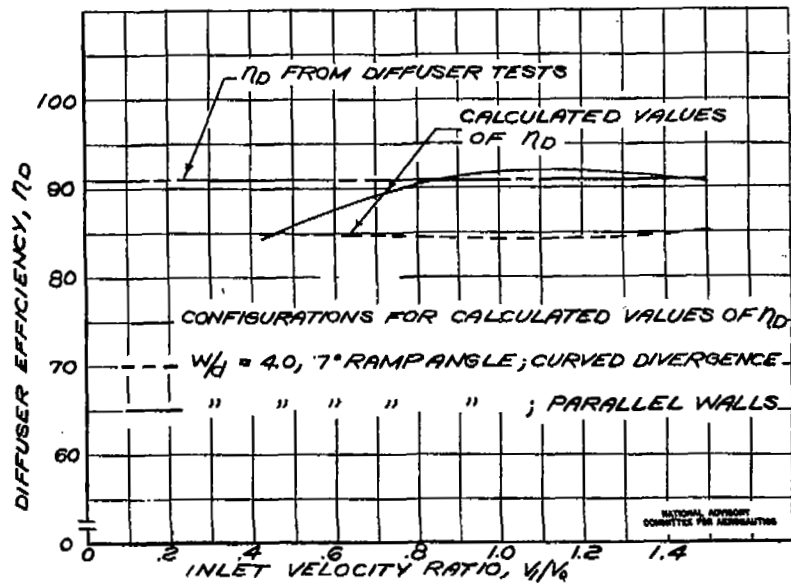


FIGURE 19.- A COMPARISON OF THE DIFFUSER EFFICIENCIES FROM BENCH TESTS WITH THOSE CALCULATED FROM THE MEASURED PRESSURE RECOVERIES.

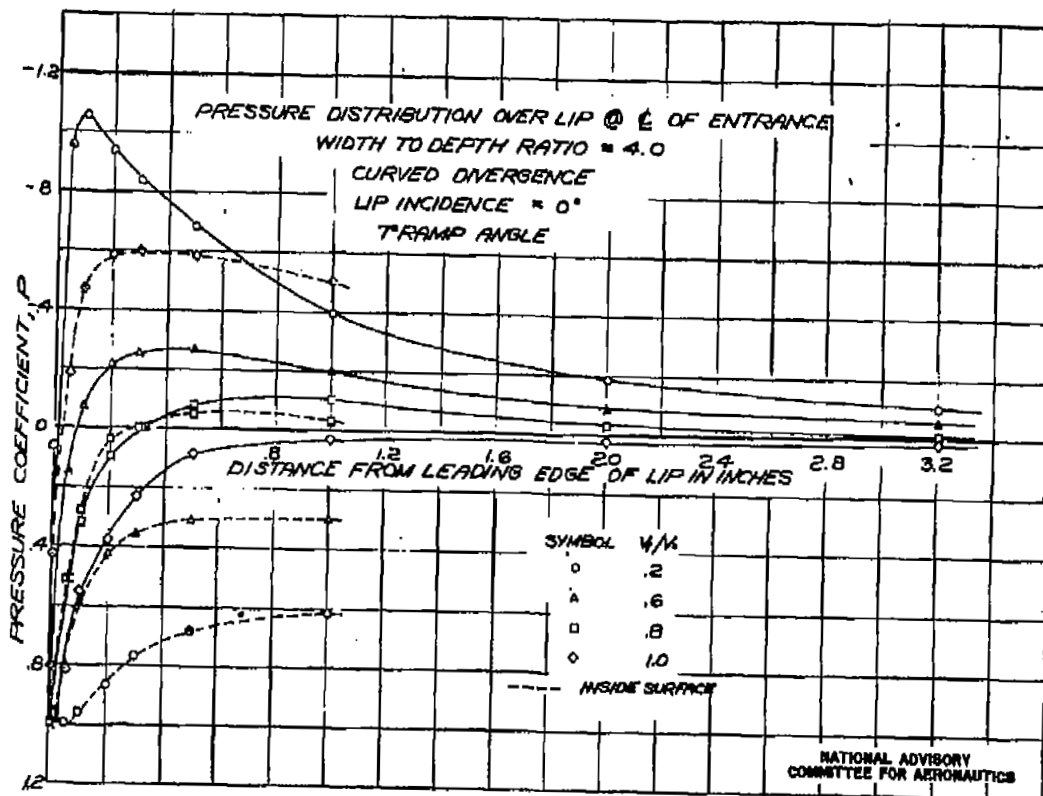
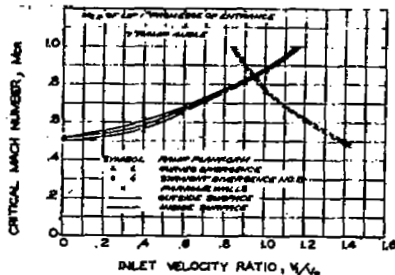
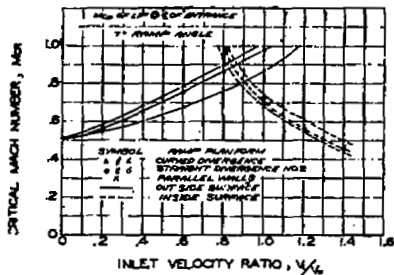
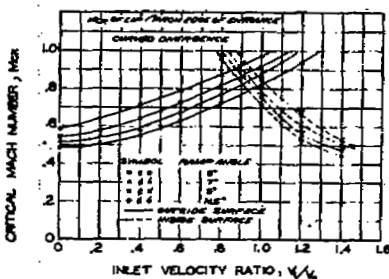
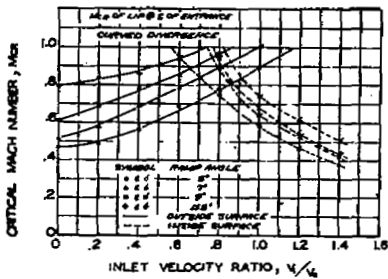
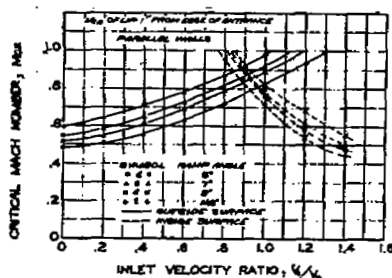
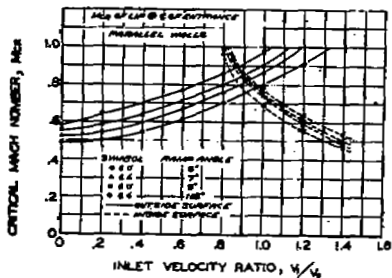


FIGURE 20.- PRESSURE DISTRIBUTION OVER THE LIP FOR VARIOUS INLET VELOCITY RATIOS.



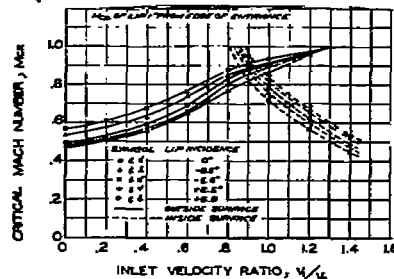
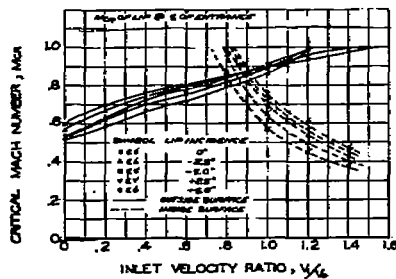
a) EFFECT OF RAMP PLANFORM



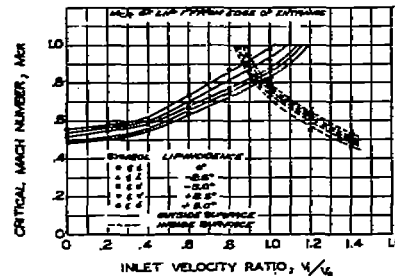
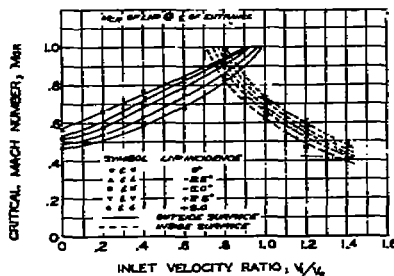
b) EFFECT OF RAMP ANGLE

NATIONAL ADVISORY
COMMITTEE FOR AERONAUTICS

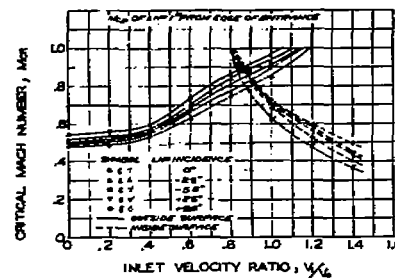
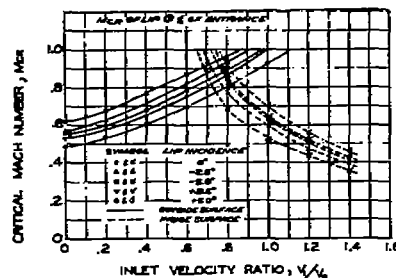
FIGURE 21. - VARIATION OF CRITICAL MACH NUMBER OF THE LIP WITH INLET VELOCITY RATIO FOR VARIOUS INLET CONFIGURATIONS. $\gamma/d = 4$, LIP INCIDENCE = 0°



a) $\frac{b}{d} = 2$



b) $\frac{b}{d} = 4$

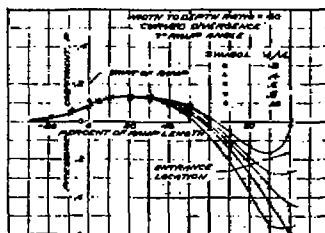


c) $\frac{b}{d} = 6$

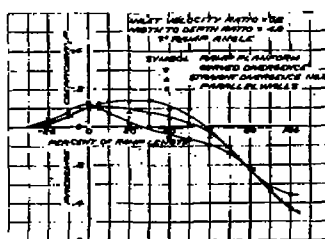
NATIONAL ADVISORY
COMMITTEE FOR AERONAUTICS

FIGURE 22.- THE EFFECT OF LIP INCIDENCE ON THE VARIATION OF CRITICAL MACH NUMBER OF THE LIP WITH INLET VELOCITY RATIO FOR THREE WIDTH TO DEPTH RATIOS OF THE ENTRANCE. CURVED DIVERGENCE, γ RAMP ANGLE.

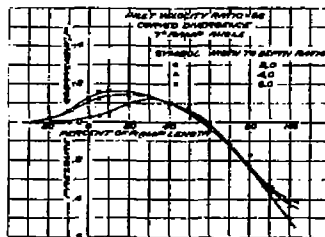
~~Handwritten scribble~~



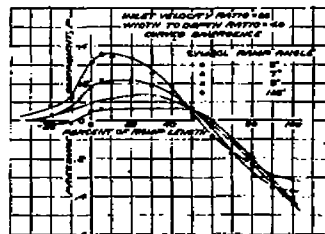
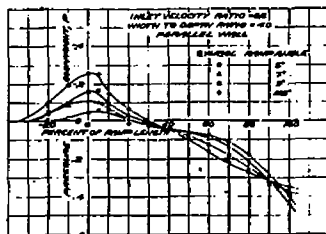
(b) EFFECT OF INLET VELOCITY RATIO



(b) EFFECT OF RAMP PLAN FORM



(c) EFFECT OF w/d OF THE ENTRANCE

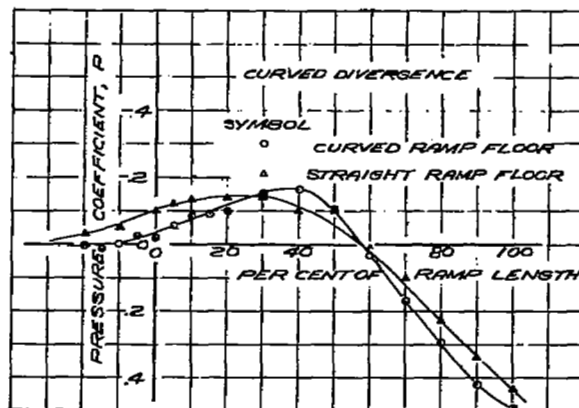
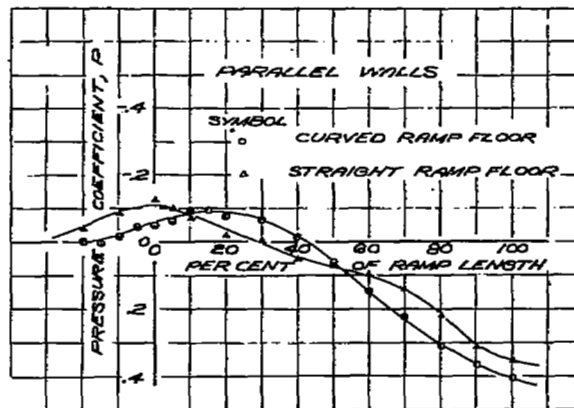


(d) EFFECT OF RAMP ANGLE

NATIONAL ADVISORY
COMMITTEE FOR AERONAUTICS

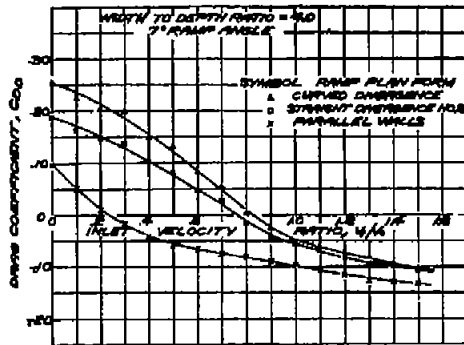
FIGURE 23.- THE PRESSURE DISTRIBUTION ALONG THE RAMP FOR VARIOUS INLET CONDITIONS.

~~Handwritten scribble~~

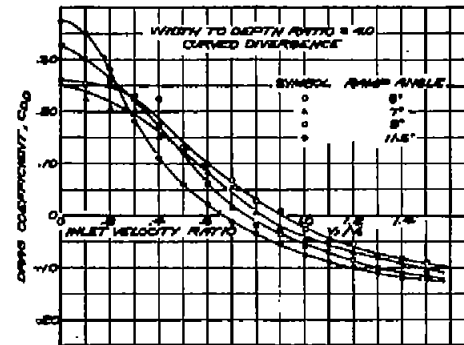


NATIONAL ADVISORY
COMMITTEE FOR AERONAUTICS

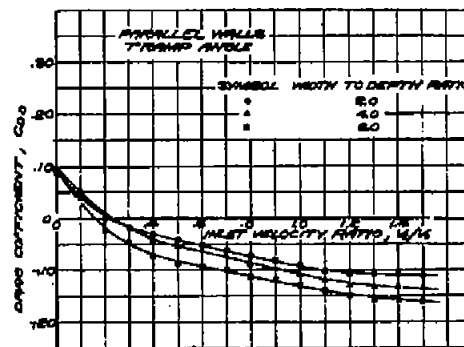
FIGURE 24.—THE EFFECT OF RAMP FLOOR SHAPE ON THE PRESSURE DISTRIBUTION OVER THE RAMP. $M_0 = 0.6$, $M_1 = 4$, T RAMP ANGLE



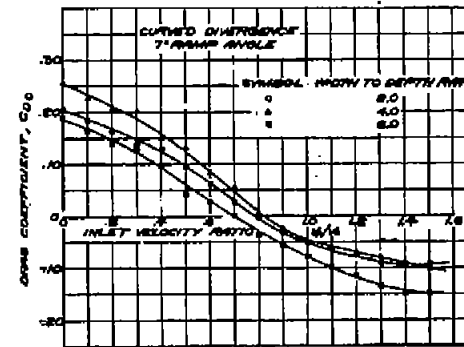
(a) EFFECT OF RAMP PLAN FORM



(b) EFFECT OF RAMP ANGLE

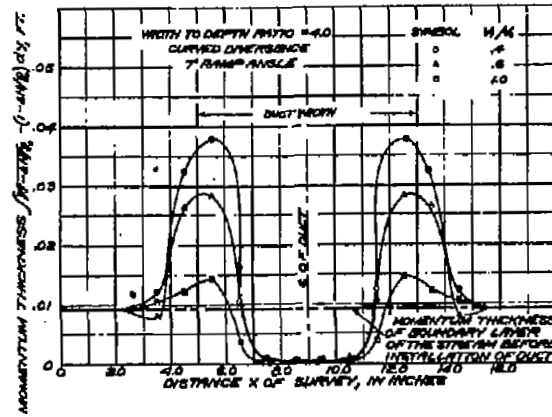


(c) EFFECT OF w/d OF THE ENTRANCE

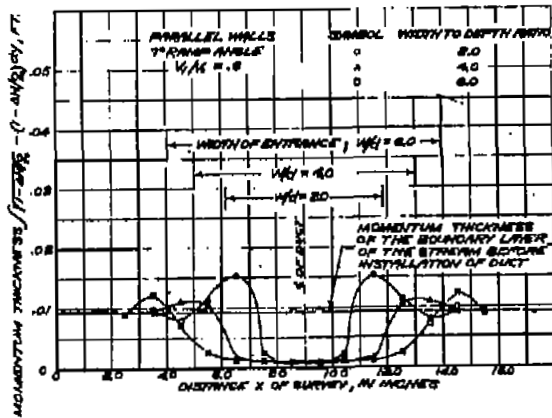


NATIONAL ADVISORY
COMMITTEE FOR AERONAUTICS

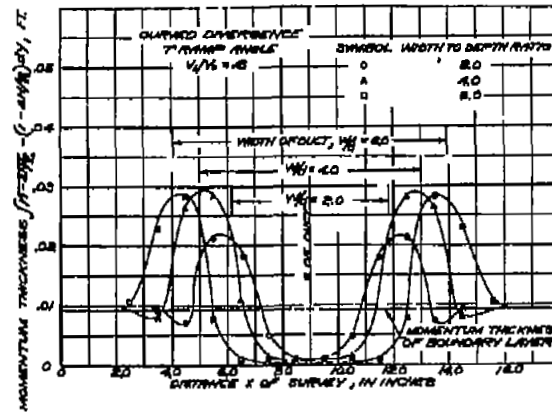
FIGURE 25-VARIATION OF THE ENTRANCE DRAG COEFFICIENT WITH INLET VELOCITY RATIO FOR VARIOUS INLET CONFIGURATIONS.



(a) EFFECT OF INLET VELOCITY RATIO

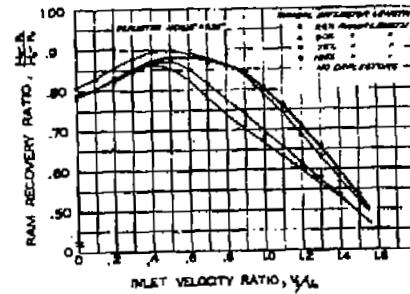
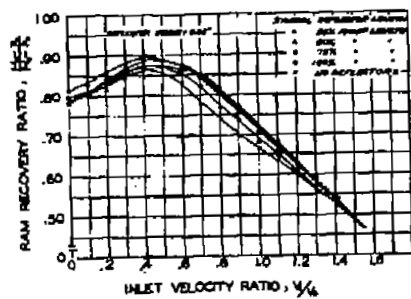


(b) EFFECT OF w/d OF THE ENTRANCE

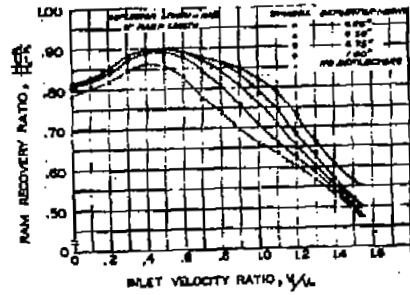
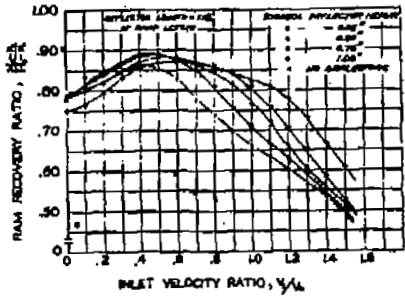
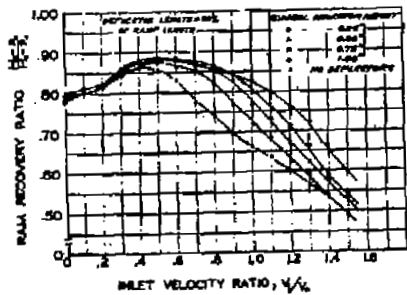


NATIONAL ADVISORY
COMMITTEE FOR AERONAUTICS

FIGURE 26.-THE DISTRIBUTION OF THE LOSS IN MOMENTUM, IN TERMS OF MOMENTUM THICKNESS, OF THE FLOW DOWNSTREAM OF THE SUBMERGED ENTRANCE FOR SEVERAL INLET CONDITIONS.



a) EFFECT OF DEFLECTOR LENGTH



b) EFFECT OF DEFLECTOR HEIGHT

NATIONAL ADVISORY
COMMITTEE FOR AERONAUTICS

FIGURE 27 - THE EFFECT OF DEFLECTOR SIZE ON THE VARIATION OF RAM RECOVERY RATIO, MEASURED AFTER THE DIFFUSER SECTION, WITH INLET VELOCITY RATIO. $V/V_c = 4$, CURVED DIVERGENCE, RAMP ANGLE 7° .

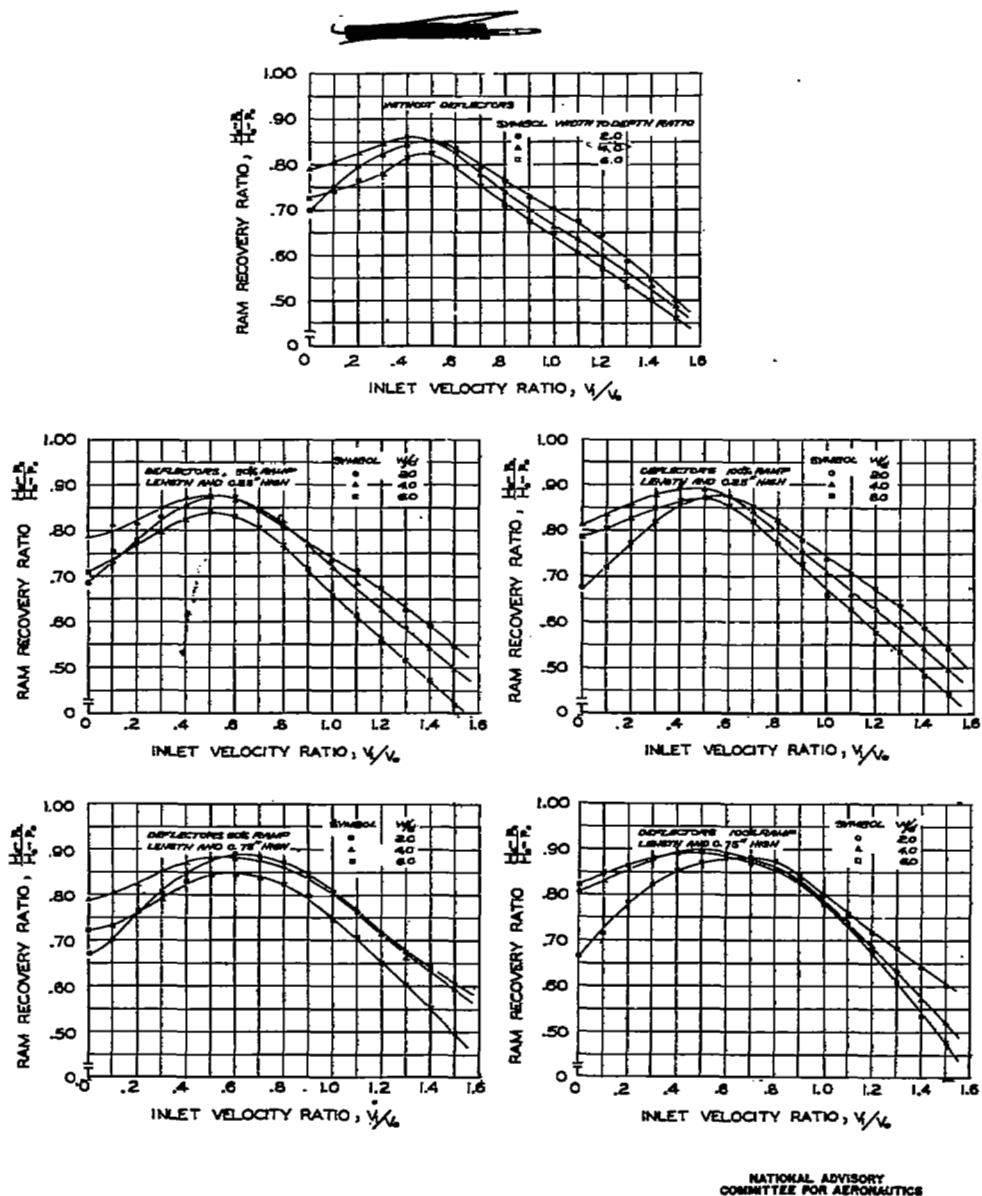
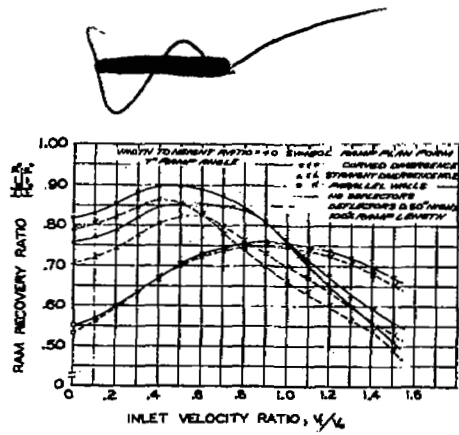
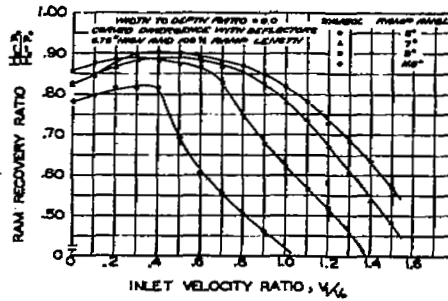
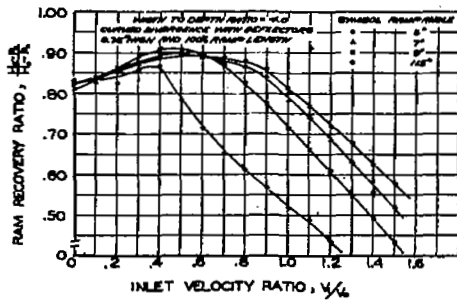
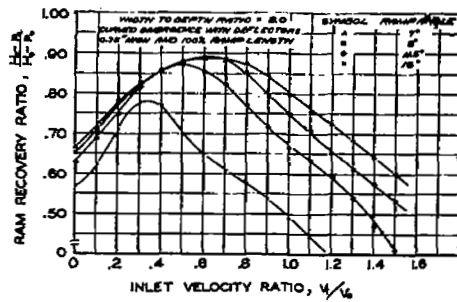


FIGURE 28. - THE EFFECT OF DEFLECTORS ON THE VARIATION OF RAM RECOVERY RATIO, MEASURED AFTER THE DIFFUSER SECTION, WITH INLET VELOCITY RATIO FOR THREE WIDTH TO DEPTH RATIOS OF THE ENTRANCE. CURVED DIVERGENCE. 7° RAMP ANGLE



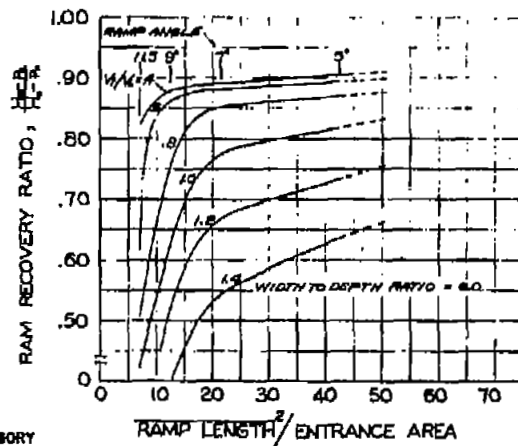
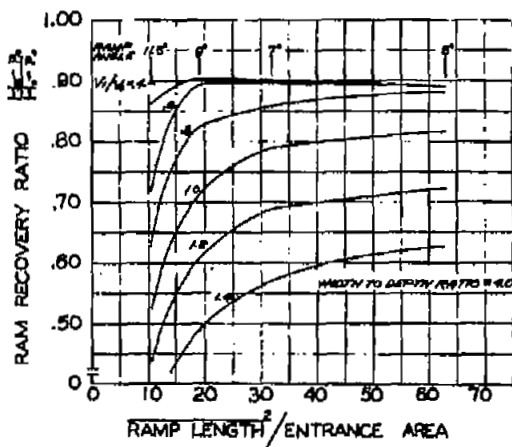
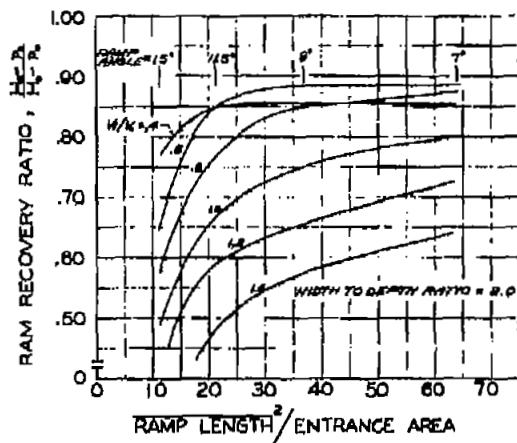
(a) EFFECT OF DEFLECTORS FOR THREE RAMP PLAN FORMS



(b) EFFECT OF RAMP ANGLE

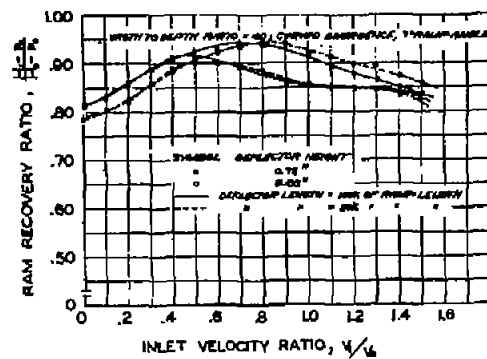
NATIONAL ADVISORY
COMMITTEE FOR AERONAUTICS

FIGURE 29.- VARIATION OF RAM RECOVERY RATIO, MEASURED AFTER THE DIFFUSER SECTION, WITH INLET VELOCITY RATIO FOR VARIOUS ENTRANCE CONFIGURATIONS WHEN DEFLECTORS ARE USED.

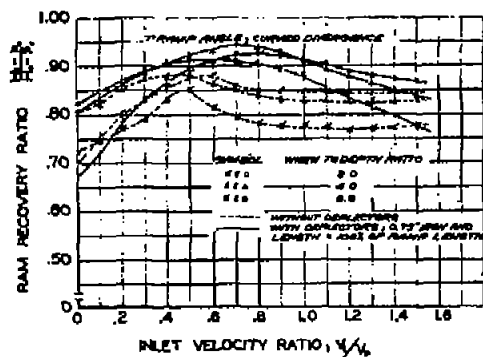
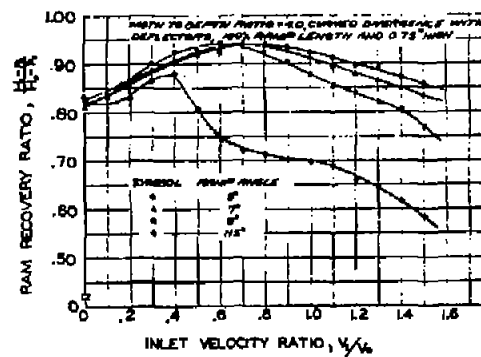


NATIONAL ADVISORY
COMMITTEE FOR AERONAUTICS

FIGURE 30. - VARIATION OF RAM RECOVERY RATIO, MEASURED AFTER THE DIFFUSER SECTION, WITH RAMP LENGTH COEFFICIENT FOR THREE WIDTH TO DEPTH RATIOS OF THE ENTRANCE. CURVED DIVERGENCE WITH DEFLECTORS, 100% RAMP LENGTH AND 0.75" HIGH.

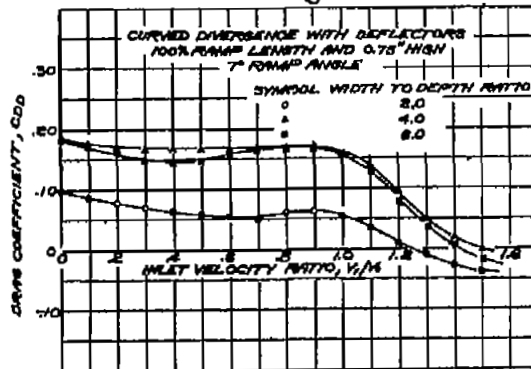


(a) EFFECT OF DEFLECTOR SIZE

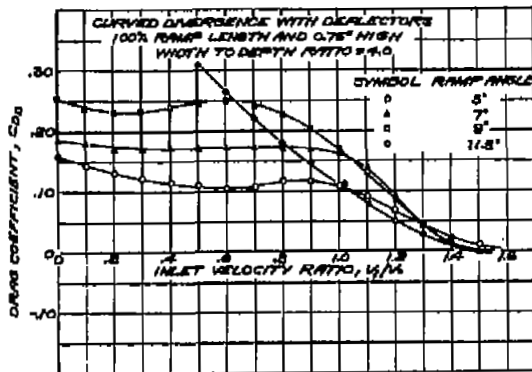
(b) EFFECT OF DEFLECTORS FOR THREE VALUES OF V_1/a .

(c) EFFECT OF RAMP ANGLE

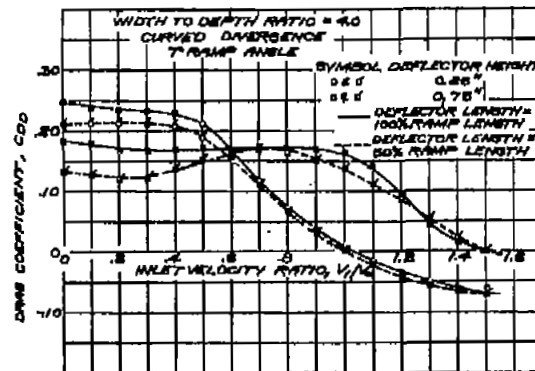
FIGURE 31.—VARIATION OF RAM RECOVERY RATIO, MEASURED AT THE SUBMERGED ENTRANCE, WITH INLET VELOCITY RATIO FOR VARIOUS ENTRANCE CONFIGURATIONS WHEN DEFLECTORS ARE USED.



(a) EFFECT OF w/d OF THE ENTRANCE



(b) EFFECT OF RAMP ANGLE



(c) EFFECT OF DEFLECTOR SIZE

FIGURE 32.-VARIATION OF THE ENTRANCE DRAG COEFFICIENT WITH INLET VELOCITY RATIO FOR VARIOUS INLET CONFIGURATIONS WHEN DEFLECTORS ARE USED.

NATIONAL ADVISORY
COMMITTEE FOR AERONAUTICS

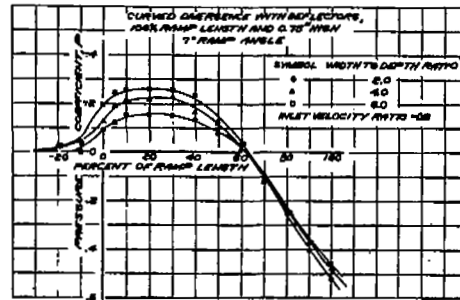
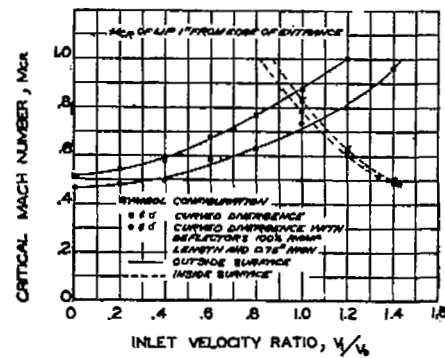
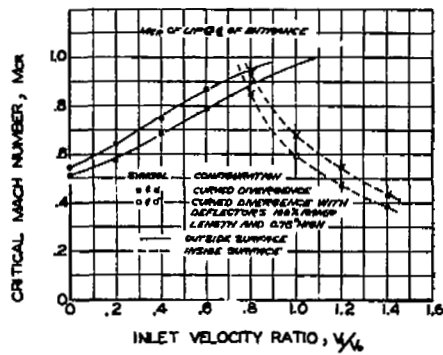


FIGURE 33 - PRESSURE DISTRIBUTION ALONG THE RAMP WHEN DEFLECTORS ARE USED.



NATIONAL ADVISORY
COMMITTEE FOR AERONAUTICS

FIGURE 34 - THE EFFECT OF DEFLECTORS ON THE VARIATION OF CRITICAL MACH NUMBER OF THE LIP WITH INLET VELOCITY RATIO.
 $R = 4$, 7° RAMP ANGLE

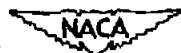
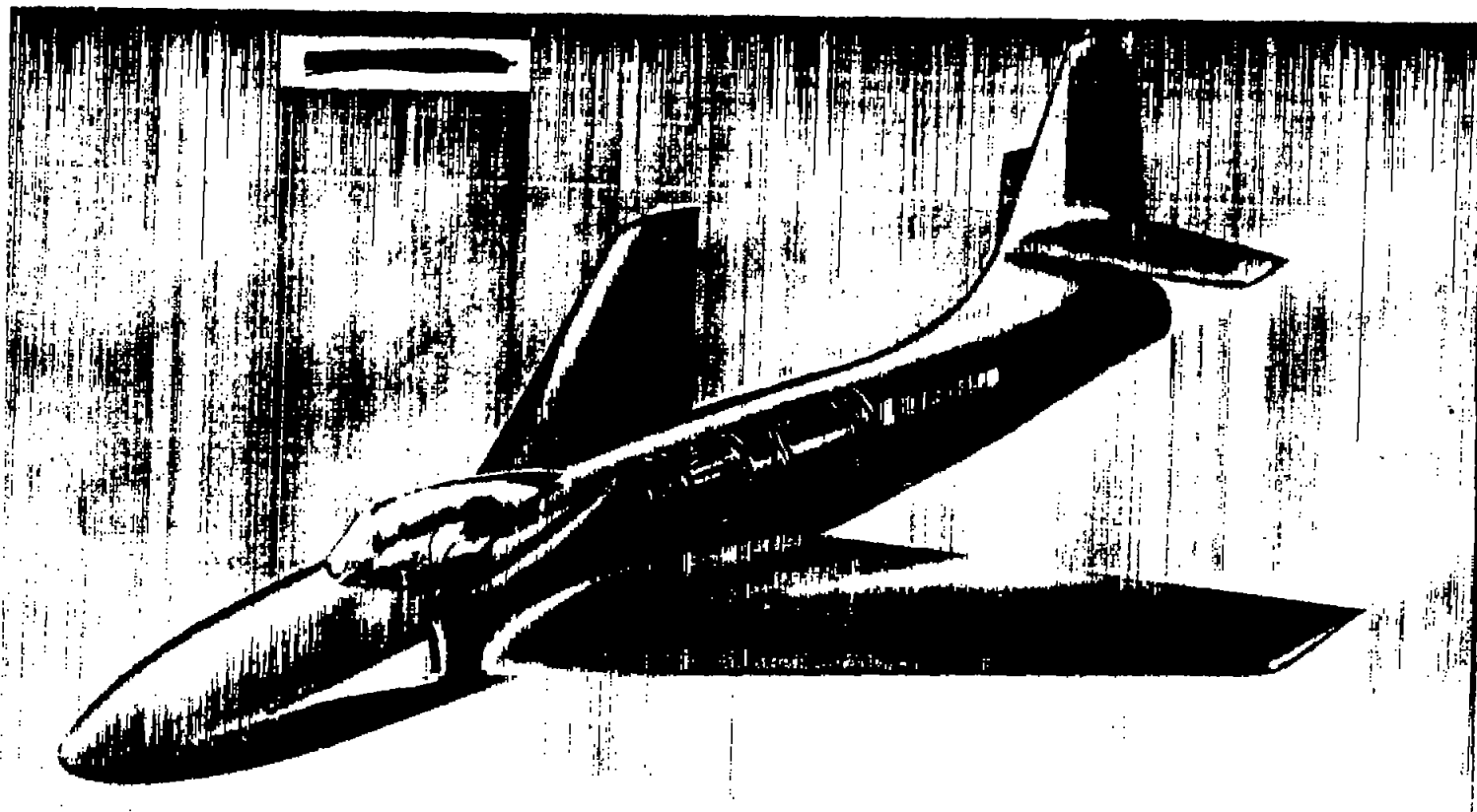


Figure 35.- A proposed installation for a single-engine jet-propelled airplane using NACA submerged air intakes.

NACA
A 11291
1-28-47.